



Virginia Commonwealth University  
**VCU Scholars Compass**

---

Theses and Dissertations

Graduate School

---

2011

## Development of Dual-Pathway Inhibitors of Raf/MEK/ERK and PI3K/Akt Signaling Pathways.

Sasha Fraser  
*Virginia Commonwealth University*

Follow this and additional works at: <https://scholarscompass.vcu.edu/etd>



Part of the [Pharmacy and Pharmaceutical Sciences Commons](#)

© The Author

---

Downloaded from

<https://scholarscompass.vcu.edu/etd/2619>

This Thesis is brought to you for free and open access by the Graduate School at VCU Scholars Compass. It has been accepted for inclusion in Theses and Dissertations by an authorized administrator of VCU Scholars Compass. For more information, please contact [libcompass@vcu.edu](mailto:libcompass@vcu.edu).

# **Development of Dual-Pathway Inhibitors of Raf/MEK/ERK and PI3K/Akt Signaling Pathways.**

A thesis submitted in partial fulfillment of the requirements for the degree of  
Master of Science at Virginia Commonwealth University.

by  
Sasha Fraser

Director: Shijun Zhang, Ph. D.,  
Medicinal Chemistry, School of Pharmacy.

Virginia Commonwealth University

Richmond.

December 2011.

## TABLE OF CONTENTS

Abstract.....	1
Literature Review .....	3
Oncogenic Signaling .....	4
Raf/MEK/ERK Pathway .....	6
Receptor Tyrosine Kinases .....	8
Non-receptor Tyrosine Kinases .....	9
Components of Raf/MEK/ERK Pathway.....	11
PI3K/ AKT Pathway.....	16
Components of the PI3K/ Akt pathway.....	18
Raf/MEK/ERK, PI3K Pathway and Apoptosis .....	19
Raf/MEK/ERK, PI3K Pathway and Cell Cycle .....	27
Signaling Dynamics.....	30
Crosstalk .....	33
Introduction .....	36
Rationale For This Study.....	36
Development of ERK 1/2 Inhibitor .....	36
Discovery of a Lead Dual Pathway Inhibitor.....	38
Objectives .....	40
Development of Oxindole as a Dual Pathway Inhibitor.....	40
Discussion and Conclusion .....	49
Anti-proliferative Assay .....	49
Western Blot Assay.....	52
Apoptotic Assay .....	53
Experimental.....	56
References .....	68

## **Abstract**

DEVELOPMENT OF DUAL-PATHWAY INHIBITORS OF Raf/MEK/ERK AND PI3K/AKT SIGNALING PATHWAYS.

By Sasha Fraser, B.Sc.

A thesis submitted in partial fulfillment of the requirements for the degree of Master of Science at Virginia Commonwealth University.

Virginia Commonwealth University, 2011.

Major Director: Shijun Zhang, Ph. D., Medicinal Chemistry.

In the present study, we designed a new chemical template that contains an oxindole moiety as potential dual-pathway inhibitors of the Raf/MEK/ERK and PI3K/Akt signaling pathways. The design hypothesis is to evaluate whether the oxindole ring system will approximately orient functional groups in a similar manner to the thiazolidinedione moiety, and thus maintain biological activity as dual-pathway inhibitors of the Raf/MEK/ERK and PI3K/Akt signaling pathways. Furthermore, the oxindole ring will provide the flexibility to allow the introduction of various substituents on the oxindole moiety, thereby facilitating comprehensive SAR studies to further explore the biological activity.

The oxindole analogs were biologically characterized by employing human leukemia U937 cells. Anti-proliferation activity using the 3-[4, 5-dimethylthiazol-2-yl]-2, 5-diphenyltetrazolium (MTT) assay was tested, and all of the designed

compounds exhibited activity against the growth of U937 cells with micromolar potency. Notably, compared to lead compound 1, the oxindole analogs, exhibited improved anti-proliferation activity (4-fold increase). Western blot analysis revealed that the expression of critical components of the pathways such as p-ERK and p-Akt, were consistently suppressed by these oxindole analogs, thus correlating the inhibition of the two signaling pathways with the anti-proliferative activity. The apoptotic effects of the most potent oxindole compounds were evaluated using flow cytometry to obtain preliminary mechanistic information. The results demonstrated that the compounds induced significant early- and late-stage apoptosis.

## **1. Literature Review**

Signal transduction pathways have long been recognized for their central role in the regulation of mammalian cellular programs in response to extracellular cues. As it pertains to the fine-tuning of important survival functions including cell cycle progression, apoptosis, and protein synthesis and growth, it is well documented that the Raf/MEK/extracellular signal-regulated kinase (ERK) and the phosphatidylinositol 3-kinase (PI3K)/Akt transduction pathways are among the key players.<sup>1,2</sup>

Notably, initial seminal studies have shown that mutations can occur at genes encoding for some of these pathway components, as well as at upstream molecules that transmit their signal through the pathways.<sup>1,3</sup> Several reports have correlated the aberrations with the induction of malignant phenotypes. Currently, it is estimated that the pathways account for more than 30% all human cancer, most often in haematopoietic malignancies.<sup>4</sup> Given the high frequency of deregulation, the pathways have been considered key targets for therapeutic intervention and, a diverse range of small molecules have been developed to the target key nodes unique to the Raf/MEK/ERK and PI3K/Akt pathways.<sup>5,6</sup> This has created a platform for a more selective targeted approach to cancer chemotherapy, a shift from the existing anti-mitotic cancer agents that crudely interfere with the basic machinery of DNA synthesis and cell division such as taxol and vinblastine.

## 1.1 Oncogenic Signaling

The dependence of transformed cells on the signaling pathways has been extensively investigated. As summarized by Hanahan and Weinberg, the current consensus is that a fully malignant invasive tumor requires deregulation of at least six physiological processes which confers:<sup>7</sup>

- Acquired self-sufficiency and independence of growth signals
- Insensitivity to growth inhibitor signals
- Circumvention of programmed cell death
- Limitless replicative potential and telomere erosion
- Sustained angiogenesis for nutrient supply
- Invasion and Metastasis

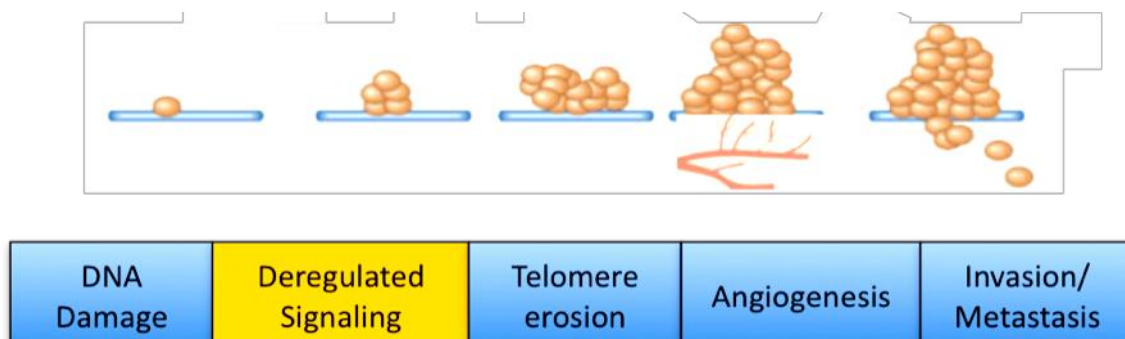


**Figure 1:** Simplified representation of the increased cell proliferation and cancer cell survival

Abnormalities in the Raf/MEK/ERK and the PI3K/Akt pathways impinge on all of these processes directly or indirectly. Generally, the constraints placed on proliferative response by the pathways are perturbed. In addition to intrinsic point mutations of signal transducer molecule such as Ras, the abnormalities include

activating mutations of RTK and chromosomal translocation, as well as over-expression of normal gene products. Although, cancers are diverse with multiple possible combinations of defects; in most cases, deregulated signaling provide the basal platform for neoplastic progression (Figure 1).<sup>3</sup> As in the case of the erosion of telomeres, although it is one of the six hallmarks of cancer, it is a result of repeated cell division. Further mutations are essentially for additional growth advantage for progeny. Angiogenesis allows development of nurturing vasculature from blood vessels of adjacent cells. The acquired self-reliance enables cell to colonize distant cells, most frequently bone and lymph node in a process termed metastasis. Due to the direct connect between uncontrolled growth and the latter complication usually leading to death; growth inhibition, cell cycle arrest and apoptosis of transformed cells is the desired endpoint of anti-cancer agents.<sup>8</sup>



## 1.2 The Raf/MEK/ERK Pathway

The Raf/MEK/ERK pathway is the prototypic pathway of the evolutionary conserved family of mitogen-activated protein kinases (MAPK)'s. It couples signals from many receptors, both membrane bound (e.g. receptor tyrosine kinases) and intracellular tyrosine kinases (e.g. ABL), to transcription factors which serve as the terminal effectors in the modulation of gene expression (Figure 2).<sup>1,4</sup>

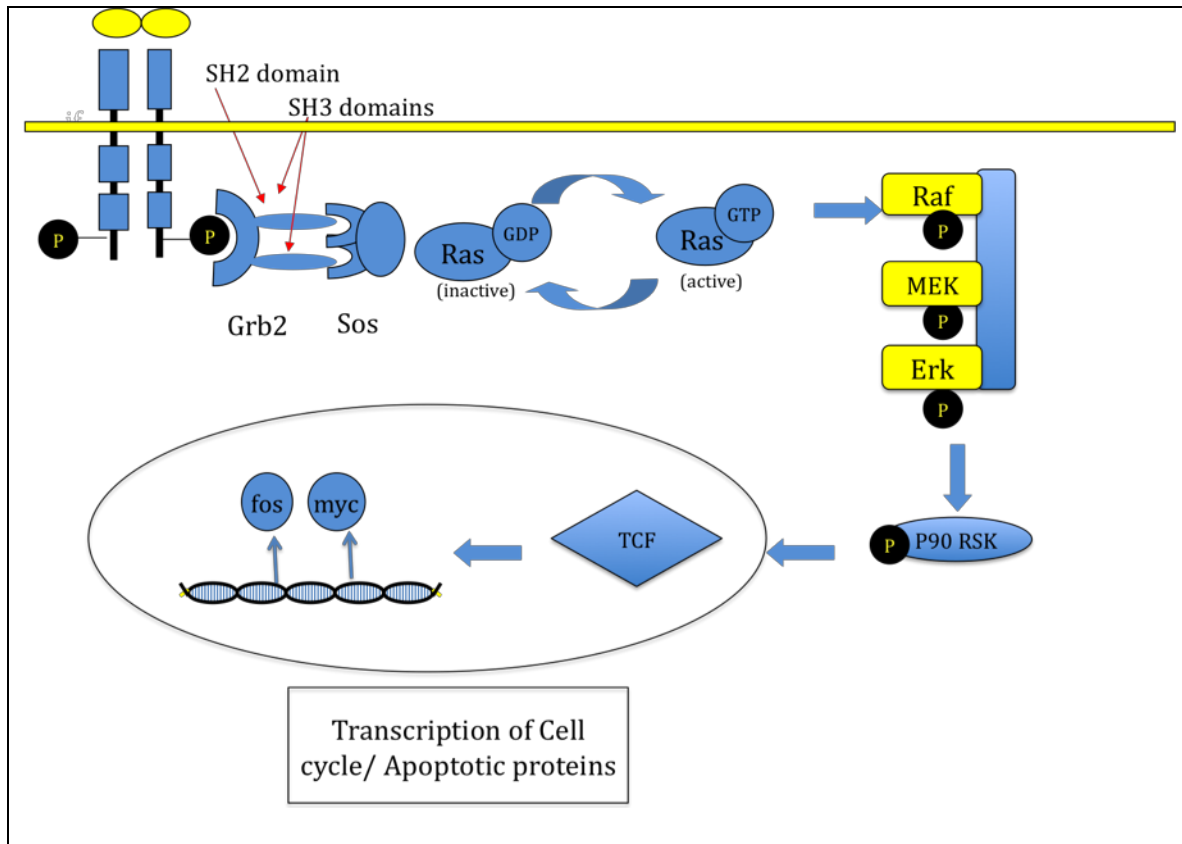


**Figure 2:** Schematic diagram of the activation of the Raf/ MEK/ ERK pathway and its downstream targets.

Historically, the Raf/MEK/ERK pathway has been synonymous with cell

cycle progression, but more recently pathway has been associated with the phosphorylation of several proteins involved in apoptosis. The core module of the pathway is three tiered and consists: Raf, a MAPK kinase kinase (MAPKKK) that can phosphorylate and activate MEK, a MAPK kinase (MAPKK), which in turn phosphorylate and activate ERK, a MAPK.<sup>9</sup> Growth factors are largely responsible for pathway stimulation. However, the pathway can be activated to some extent by ligands for heterotrimeric G protein-coupled receptors (GPCRs) and cytokines among other stimuli. The ligand-mediated activation via receptor tyrosine kinases triggers the formation of Ras in its GTP bound conformation. Subsequently, stimulating the translocation of Raf the cell membrane.

Aberrant activation of this pathway is a common occurrence. Importantly, core modules Ras and Raf were first discovered in the 1980's as transforming oncogenes of the murine sarcoma virus.<sup>10</sup> This landmark finding of the cellular origin of retroviral oncogene has contributed greatly to delineating molecular changes that drive tumorigenesis. The seminal link between the pathways and human cancers has been substantiated by 25 years of research. Several oncogenes were later found. For example, c-sis oncogene which encodes platelet-derived growth factor (PDGF), as well as oncogenes that encodes constitutively active growth factor receptor tyrosine kinases (RTKs), for example, v-erb for the epidermal growth factor receptor (EGFR) and non-receptor tyrosine kinases, for example, ABL, that relay signals through the ubiquitous Raf/ MEK/ ERK pathway.<sup>10</sup>

### **1.2.1 Receptor Tyrosine Kinase (RTK)**

The membrane-spanning receptors of the RTK family constitute a ligand-binding domain, a single trans-membrane domain and an intracellular domain with tyrosine kinase activity.<sup>11</sup> The cytoplasmic domain contains a conserved PTK domain that is subject to phosphorylation. A major requirement for signaling mediated by RTKs is ligand-induced dimerization of receptors that result in the autophosphorylation of the receptor subunits. These auto-phosphorylation sites serve to recognize the src homology 2 (SH2) of a variety of signaling proteins. One such protein is the adaptor growth factor receptor-bound protein 2 (Grb2). The second binding domain of the adaptor molecule, SH3, allows it to associate with the guanine nucleotide exchange factor (GEF), son-of-sevenless (SOS), which catalyze GDP release and GTP binding which activates Ras.<sup>12</sup>

As the first RTK to be discovered, the EFGR also known as ErbB1 homologous to the v-erb-B transforming protein of avian retrovirus is generally used as a RTK model. The EGF signal is terminated primarily through endocytosis of the receptor-ligand complex. There are various alterations that interfere with ErbB receptors functions that contribute to human cancers. Mutations are often found in the intracellular domain which affects tyrosine kinase activity and abrogates the requirement for growth factor signals. In some tumors, increased production of EGF-related growth factors leads to the persistent activation of ErbB receptors. Similarly, over-expression of receptor, and oligomerization mimics of EFGR and other RTKs have been implicated in numerous cancers including ovarian and gastric carcinomas and glioblastoma.<sup>13</sup>

### **1.2.2 Non-Receptor tyrosine kinase**

The non-receptor kinases are key elements of intracellular signaling induced by extracellular stimuli, such as cytokines and growth factors. These proteins are localized both in the nucleus and cytoplasm, and regulate cell growth, survival and morphogenesis via the PI3K/Akt and the Raf/MEK/ERK pathways. The family of Abelson murine leukemia virus (c-Abl) tyrosine kinase has gained much interest since the finding that a single molecular abnormality can cause transformation of a hematopoietic progenitor into a malignant clone. Similar to its receptor counterpart, c-Abl was originally identified as the cellular homolog of the v-Abl oncogene of the Abelson murine leukemia virus, and its function depends on its kinase activity, which is believed to involve phosphorylation of Tyr245 and Tyr412.<sup>14</sup>

Abnormality of the Abl protein through the reciprocal translocation between the ABL chromosome 9 and chromosome 22 near a locus termed the break-point cluster region (BCR) is the primary mode of deregulation in CML. The result is a constitutively active ABL tyrosine kinase domain which abrogates the need for activation by other cellular messaging proteins. This BCR-ABL transcript, also called the Philadelphia chromosome (Ph<sup>+</sup>) accounts for more than 95% of hematopoietic malignancies.<sup>15</sup> Interestingly, in the stable or chronic phase of CML while there is a massive increase in the number of white blood cells, their maturation and function of the white blood cells are normal until a malignant clone loses its ability to differentiate resulting in disease progression to highly refractory leukemia.

### 1.2.3 Ras

Ras is a notable member of the GTPase superfamily (also known as guanine nucleotide binding proteins), and it is a critical link that allows signal transduction from the tyrosine kinases. Three isoforms have been identified (*H-Ras*, *N-Ras* and *K-Ras*). These proteins are typically anchored on the cytoplasmic face of plasma membrane by farnesylation, where they cycle between GTP-bound and GDP-bound state acting as a binary switch for several signaling pathways including the Raf/MEK/ERK and the PI3K/Akt pathways. It has been shown that there is specificity in the capability of isoforms to activate the pathways; K-ras preferentially activates the Raf/MEK/ERK pathway whereas K-Ras activates the PI3K/ Akt pathway.<sup>9</sup>

Localisation at the cell membrane allows the Ras proteins to be positively regulated by guanine nucleotide exchange factor such as SOS which promotes GDP dissociation. Consequently, the nucleotide free binding pocket will bind GTP since its concentration in the cytosol is ten-folds higher than that of GDP, markedly changing the conformation of the switch 1 and switch 2.<sup>16</sup>

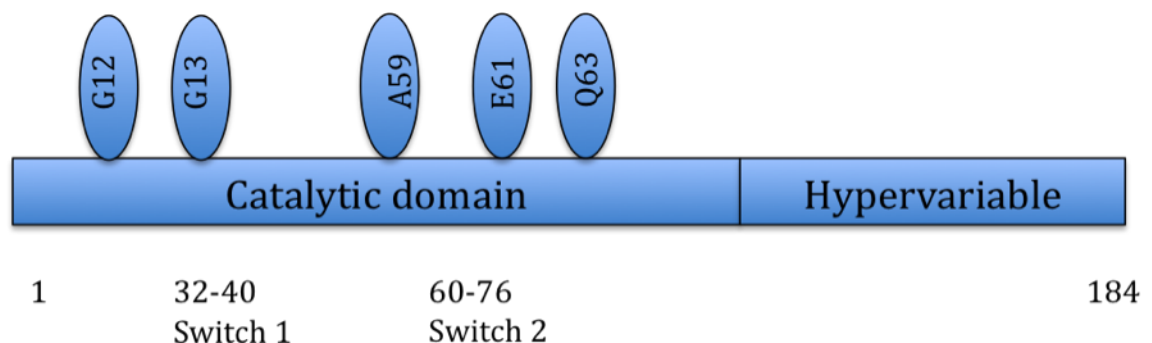


**Figure 3:** The sites of mutations detected in Ras are indicated. These mutations at (12, 13, 59, 61, 63) locks the Ras protein in an active state, which cannot be inactivated by the GTPase.

Damage to these small GTPases switches can have catastrophic effects. The Ras mutants are ranked among the most potent transforming proteins known, accounting for 30% of all cancers, with pancreas (90%), thyroid (60%) and colon cancer (50%) having the highest prevalence.<sup>17</sup> The activation of the mutant Ras genes is invariably by point mutation at the codons: 12, 13, 59, 61 and 63 (Figure 3).<sup>18,19</sup> These activating mutations stabilize the GTP-bound state and impair the GTPase activity of Ras, locking the Ras protein into its active conformation. Within the ERK signaling pathway, active Ras binds the effector Raf kinase, stimulating their translocation to the cell membrane, where Raf activation takes place.

#### **1.2.4 Raf**

The Raf serine/ threonine kinases lie at the apex of the Raf/MEK/ERK pathway module, and exist as the isoforms: A-Raf, B-Raf, and Raf1. These proteins have three functional domains: CR1, CR2 and CR3 (Figure 4). The CR1 domain is necessary for Ras binding and activation. The CR2 domain is the regulatory domain, and the CR3 is the kinase domain. Although these isoforms share several structural features they exhibit non-redundant functions and differ considerably in their modes of regulation.<sup>7,19</sup>

The recruitment to the cell membrane by GTP-bound Ras is the initiating event and full activation of Raf-1 follows a complex sequence of (1) phosphorylations/ dephosphorylations, (2) protein-protein interactions, and (3) lipid/ protein interactions.<sup>17</sup> These events enhance the catalytic activity of Raf1

by both facilitating the activation of the kinase domain and neutralizing auto-inhibitory molecules. The auto-inhibitory conformation state is maintained by 14-3-3 dimers, and relief from auto-inhibitory molecule entails dephosphorylation at S259 by the serine threonine phosphatases (PP2A). This allows Raf-1 to assume a new conformation in which it can be phosphorylated at S338, and activated by kinases including P21 activated protein kinases (PAK).<sup>20</sup>

The S259 and S338 sites of Raf-1 are conserved in A-Raf which follows a similar activation patterns to Raf-1. However, B-Raf has two aspartate residues at the position equivalent to S338 making the protein constitutively active due to the negative charge of the aspartate. As a result B-Raf can be sufficiently activated by Ras only, while Raf 1 requires other factors.

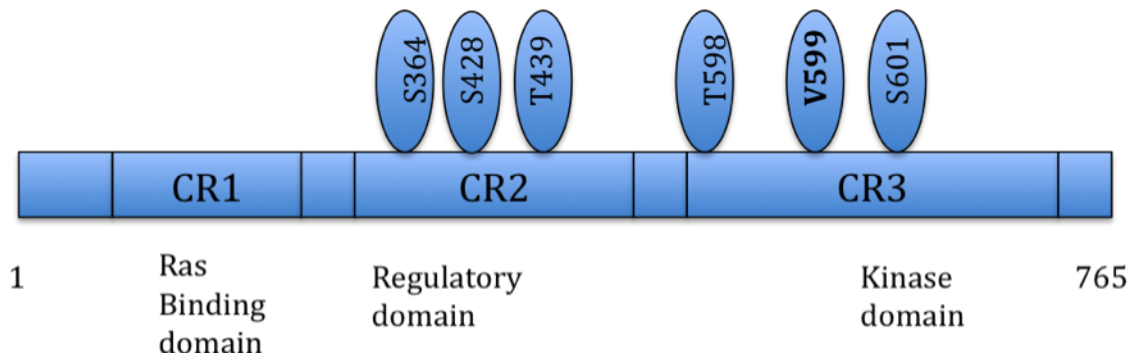


**Figure 4:** The sites of mutations detected in the B-Raf protein are presented. In all, 90% of B-Raf mutations in melanoma involve V599. Mutations at S364, S428 and T439 insulate connectivity to the PI3K/ Akt pathway.

B- Raf is the most oncogenic isoform. B- Raf mutations have been reported in 66% of melanoma, 53 % of thyroid cancer and 30% of ovarian cancer.<sup>5</sup> The activating mutations within the kinase domain are the most aggressive, and often converts Val599 to Glu. Interestingly, B-Raf mutations confer low kinase activity. The recent discovery that B-Raf can form heterodimers with Raf-1 is a point of

high interest. Recently, it has been shown that B-Raf can activate Raf-1. The kinase activity of the B-Raf/ Raf-1 heterodimer is considerably higher than the ability of either B-Raf or Raf-1 as independent entities. It is believed that heterodimerization between B-Raf and Raf-1 proteins may allow the impaired B-Raf to activate Raf-1.<sup>21</sup>

#### **1.2.5 Mitogen-activated Protein/Extracellular Signal-regulated Kinase (MEK)**

MEK proteins are the most relevant target of Raf. This family of dual-specificity kinases has both S/T and Y kinase activity. Their structure constitutes a regulatory domain and a MAP kinase-binding domain necessary for binding and activation of ERKs. Surprisingly, there has been no identified oncogene derived from MEK. MEK also differ from the upstream molecules Ras and Raf in that it has relatively few phosphorylation sites.

MEK's activity is positively regulated by Raf kinase through phosphorylation at Ser 218 and serine 222.<sup>21</sup> MEK can be partially activated by phosphorylation at either site. There are several featured MEK inhibitors that block ERK activity by a noncompetitive mechanism, by binding in a pocket adjacent to but not overlapping the ATP binding site. While this feature is desirable, the demise of the MEK inhibitors is the high frequency of crosstalks upstream MEK that can circumvents signaling beyond MEK.



### **1.2.6 Extracellular signal-regulated kinases (ERK)**

The main physiological substrates of MEK are the ERK family of serine/threonine and tyrosine kinases of the Raf/MEK/ERK pathway, expressed in all mammalian tissue, with ERK2 levels generally higher than ERK1. Dual phosphorylation activates both at T202/Y204 for ERK 1 and for T185/Y187 ERK2 in humans within a conserved Thr-Glu-Tyr (TEY) motif in their activation loop. Unlike MEK, ERK activation requires phosphorylation at both sites for full activity, and Tyr phosphorylation has been shown to precede Thr phosphorylation.<sup>22</sup>

Both nuclear and cytoplasmic have been identified for ERK. Activated Erk can phosphorylate cytoplasmic signaling proteins including P90 ribosomal S6 kinase (RSK). ERK can also translocate to the nucleus, where it directly phosphorylates member of the TCF family, for example Elk-1. TCF activate numerous immediate early genes (IEG) including c-fos and c-myc that binds the promoter of many genes. Accordingly, phosphorylation of TCF potentiates the ability of IEG products to modulate the expression of many other genes including cyclin D1; thereby, facilitating G1/S transition in the cell cycle.<sup>4, 23</sup>

To date, over 160 substrates have identified.<sup>24</sup> The apparent specificity and efficiency within the MAPK signaling is partly achieved through docking motifs, namely, the D, DEF, CD, and ED domains which are present in scaffolding proteins such as KSR. While the D domains are recognized generally by the family of MAPKs, the second domain termed DEF (docking site for ERK and FXFP), that consists of the Phe-Xaa-Phe-Pro sequence has been reported to be recognized only by ERK1/2 in the C-terminal of the phosphoacceptor site. Also at

the C-terminal is the conserved common docking motif outside the catalytic domain which contains acidic and hydrophobic residues necessary for hydrophobic and electrostatic interaction with residues of the D-domain. Similar to the D motif, the ED motif is adjacent the catalytic center of Erk which is also believed to contribute to substrate binding specificity.<sup>25</sup>

### 1.3 The PI3K/Akt Pathway

Similar to ERK pathway, the engagement of several different growth factors with RTKs feed into the PI3K/ AKT pathway. The net effect is the inhibition of the apoptosis and stimulation cell cycle progression and cellular translation. Germane to survival signaling the class 1a PI3K kinases triggers the production of the second messenger phosphatidylinisitol 3,4,5-triphosphate (PIP3). PIP3 activates central engine of the pathway, AKT, which in turn modulates several downstream signaling proteins (Figure 5).<sup>20, 26, 27</sup>

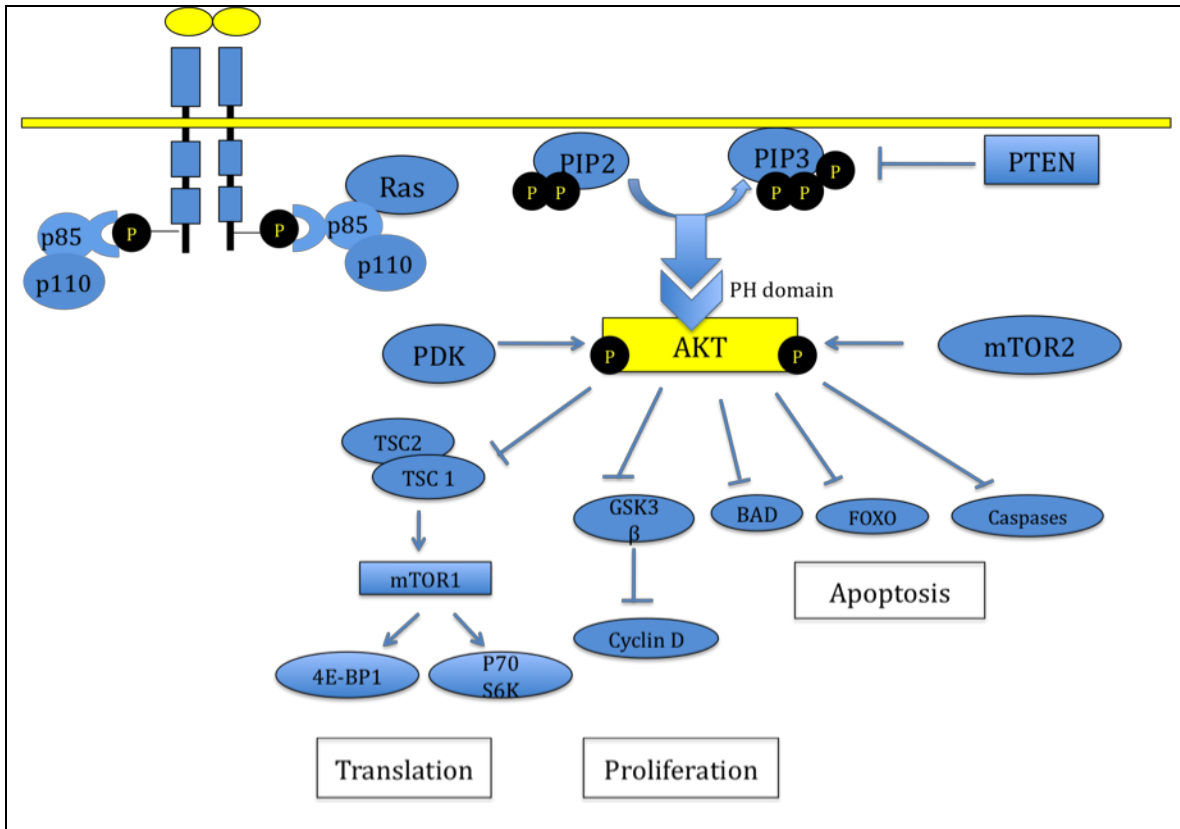


**Figure 5:** Schematic diagram of the activation of the PI3K pathway and a number of critical downstream targets.

One of the most important AKT substrate is mTOR which allow the pathway to mediate a key step in translational control. The classical thought was that the pathway discretely exerts anti-apoptotic effects through phosphorylation of critical targets including FOXO, BAD and caspases. However, recent studies also indicate that Akt also promotes cell cycle progression by its ability to phosphorylate MDM2 and GSK-3. Though, the connection between its role in apoptosis and cell cycle is not entirely clear p53 seem to be involved.<sup>1</sup>

Insult to the PI3K/ AKT pathway has been implicated tumorigenesis. The importance of PI3Ks in cancer was confirmed by the discovery that the PI3K catalytic subunit alpha-isoform gene (PIK3CA), which encodes p110 $\alpha$ . Other defects in the pathway may include AKT are overexpression, and the negative regulators of the pathway such as the tumor suppressor, PTEN may be mutated or absent.<sup>28,29</sup>

### **1.3.1 Phosphoinisitol Kinase (PI3K)**

The PI3K proteins are a family of lipid kinases that serve to phosphorylate the 3-hydroxy group of phosphoinisitol. These PI3K proteins are cytoplasmic heterodimers composed of a one of several p110 catalytic subunits, such as PIK3Ca and PIK3Cb, and a regulatory p85 protein. The RTKs can activate the PI3K pathways by two mechanisms. This may be directly through the binding of the SH2 domain of p85 regulatory subunit of PI3K to specific phosphotyrosine residue of the activated RTK.<sup>30</sup> Alternatively, RTK may bind the adaptor proteins which activate Ras inducible membrane translocation and activation of p110

catalytic unit of PI3K.<sup>31</sup> The activated PI3K phosphorylates phosphatidylinositol-3,4-bisphosphate (PIP2) to generate the secondary phosphatidylinositol-3,4,5-triphosphate (PIP3). Subsequent signaling from the PI3k Ia is mediated primarily through the recruitment of protein containing PH domain including PDK1 and AKT, to the 3' phosphoinositides. The membrane bound phospholipid, PIP3, acts as a docking site to bring the Akt from the cytosol to the plasma membrane in closer proximity to (PDK1) poised for activation.

The contribution of PI3Ks to cancer progression was confirmed by the discovery of the mutated PI3K catalytic subunit, alpha-isoform gene (PIK3CA), which encodes p110 $\alpha$ . Three of the most frequent PIK3CA mutations, E542K, E545K in the helical domain incur a charge reversal that inhibits electrostatic interactions between the inserted amino acids and R340 and K379 on the SH2 domain of regulatory p85 $\alpha$  (Figure 6). H1047R in the kinase domain, have been shown to increase PIP3 levels. It has been proposed that R forms a hydrogen bond with L956 of p110 $\alpha$ , which in turn leads to catalytic activity of p110 $\alpha$ .<sup>32</sup> Cumulatively, studies indicate that the gain of function in helical domain mutations is independent of binding to the regulatory p85 but requires binding to RAS-GTP. In contrast, the kinase domain mutation is active in the absence of RAS-GTP binding but is highly dependent on the interaction with p85. Colorectal, brain and gastric cancers are reported to have a high rate of PIK3CA gene mutation with frequencies of 32%, 27% and 25%, respectively.<sup>29</sup>

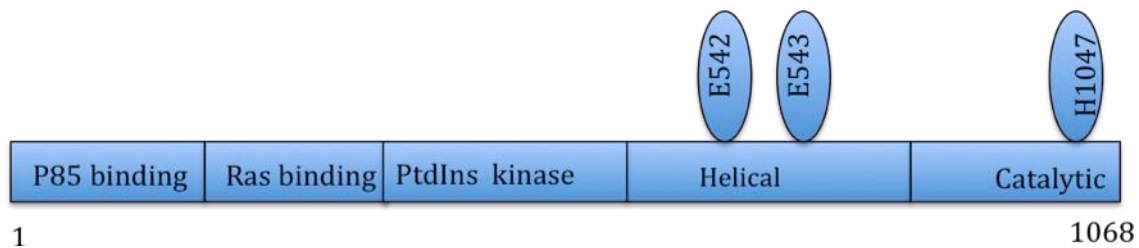


**Figure 6:** Mutations of the PIK3CA gene of the catalytic p110 domain in the helical domain: E542K and E543 K, and in the catalytic domain H1047.

### 1.3.2 Akt

The AKT/ PKB serine/ threonine kinases are the principal target of the PI3K pathway. Similiar to Ras, Akt was discovered as the cellular gene of the transforming retrovirus AKT8 which exhibited kinase properties similar to protein kinases A and C. It is expressed in three isoforms: Akt1, Akt2, and Akt3, all of which possess an N-terminal pleckstrin homology (PH) domain involved in lipid binding, a kinase domain and a regulatory C-terminal tail. Akt is activated via phosphorylation of two residues: T308 and S473.<sup>33</sup> PIP3 facilitates the phosphorylation of AKT at T308. An additional phosphorylation in the C-terminal at S473 is also required for full activation, and the mammalian target of Rapamycin 2 (mTOR 2) complex is believed to have some role, but the precise mechanism remains controversial.

Activated Akt phosphorylates and stimulates many survival factors. It promotes protein synthesis and growth by activating mTOR1 through effects on the intermediary tuberous sclerosis (TSC) 1/2 complex. Akt influences apoptosis by phosphorylating molecules such as BAD and BIM. Moreover, Akt can modulate cell cycle progression via regulation of GSK-3 and MDM2 activity which

regulates cyclin D and myc.<sup>1</sup> A recent report identified a somatic mutation in the PH domain of AKT1 (E17K) in 8% of breast cancers. The acidic Glu 17 typically forms an ionic interaction with basic Lys 14 in the pocket however, in the case of the Lys 17 substitution in E17K, the positively charged Lys 17 can no longer interact with Lys 14. Consequently, the mutated AKT1 product is recruited to the membrane through a PI3K-independent mechanism.<sup>1, 34</sup>

### **1.3.3 Mammalian Target of Rapamycin 2 (mTOR)**

Integral to the translation of cell growth proteins in mammals is the murine target of rapamycin mTOR, a multidomain serine/ threonine kinases known to be inhibited by the drug rapamycin. As the downstream target of Akt, mTOR is activated by Akt-induced phosphorylation of the intermediary tuberous sclerosis complex2 (TSC2). The main function of mTOR is the regulation of translation, particularly the recruitment of ribosomes to mRNA. Several survival proteins possessing a tertiary structure with polypyrimidine stretch in their 5' untranslated region (UTR) are difficult to translate, and relies on mTOR for efficient translation. This requires the assembly of a translational complex that attaches to 5' UTR. The translation complex comprises eIF4E which recognize the cap structure at the 5' end of mRNA, RNA helicase eIF4A and its activator eIF4B which serves to unwind the 5' UTR structure, all of which collaborates to allow the 40S ribosomal subunit binding.<sup>1,35</sup>

The activation of mTOR requires the association with Ras homologue enriched in brain (Rheb) in its GTP form. The tuber schlerosis complex (TSC 1 /2) is the key integrator of PI3K/ mTOR signaling, and acts by promoting Rheb

GTPase activity which negatively regulate mTOR activation. However, TSC1/2 is inhibited by PI3K signaling. The activated mTOR complex exerts its effect through phosphorylation of ribosomal p70S6 kinase (S6K1) and the eukaryotic initiation factor 4E (eIF4E)-binding protein 1 (4E-BP1).<sup>1</sup> 4E-BP1 is known to inhibit 5'cap-dependent mRNA. The phosphorylation of 4E-BP1 releases eIF4E to facilitate the mRNA binding to the ribosome and translation initiation. The phosphorylation of 4E-BP and the free eIF4E generally stimulate two-fold increase in translation. However the translation of specific protein such as c-myc containing high structured UTR can be significantly larger. S6K1, in a more indirect manner acts on many substrate including RNA helicase and other substrates involved in translation. Both substrates stimulate the translation of proteins necessary for cell growth and division of protein such as c-myc and cyclin D.<sup>35</sup>

#### **1.3.4 Phosphatase and Tensin homolog deleted on chromosome 10 (PTEN)**

The PI3K pathway is negatively regulated by the tumor suppressor protein phosphatase and tensin homolog deleted on chromosome 10 (PTEN). The lipid phosphatase serves to check and maintain balance between PIP2 and PIP3 by degradation of PIP3 through the removal of the phosphate group from the 3' position of the inositol ring. PTEN is ranked among the most common mutated tumor suppressors in human cancers, second only to p53 mutations. The immediate consequence of loss of function is increased levels of PIP3 and up regulation of a number of AKT regulated proteins.<sup>36</sup>



#### **1.4 The Raf/MEK/ERK, the PI3K/Akt Pathways and Apoptosis**

The Raf/MEK/ERK cascade and the PI3K/Akt cascade have been demonstrated to control the activity of several proteins involved in apoptosis. Of the two modes of apoptotic regulation, designated as receptor mediated and the mitochondrial mediated, the mitochondrial mode is thought to be the principal target of survival signaling pathways. The Bcl-2 protein family is largely responsible for this mode of regulation. The BH3-only members including Bad and Bim, are essential initiators of apoptosis activated in response to distinct cytotoxic and developmental signals. They selectively bind to pro-survival members of the Bcl-2 family such as Bcl-2, Bcl-xL to trigger the mitochondrial release of cytochrome c by a mechanism requiring their pro-apoptotic relatives Bax or Bak (Figure 7). It is believed that the balance of the antiapoptotic proteins and the pro-apoptotic proteins dictates cell survival or apoptosis.<sup>13, 37</sup>

The BH3-only protein (B-Cell CLL/ lymphoma 2 (Bcl-2)/ Basal cell lymphoma-extralarge (Bcl-xL) associated promoter (BAD) was the first pro-apoptotic Bcl-2 family member found to be regulated by extracellular survival signaling. In cells stimulated with mitogens, such as EGF, Bad is phosphorylated at S136 by AKT. Several other reports indicate that RSK and S6K can both phosphorylate BAD at S112.<sup>38</sup> These phosphorylation events on apoptotic regulatory molecules affect their stability, and alter their subcellular distribution. Input from both pathways inhibits the pro-apoptotic activity of BAD by allowing recognition by, and subsequent interaction with the 14-3-3 scaffold protein in the cytosol. The BAD-14-3-3 heterodimer promotes cell survival by sequestration of

BAD in the cytosol where it is spatially separate from the mitochondria and pro-apoptotic members of the Bcl-2 family. Conversely, upon withdrawal of mitogens, hypophosphorylated BAD induce oligomerization of Bak and Bax. Activated BAX/BAK dimer induces mitochondrial outer membrane permeabilization (MOMP) release as cytochrome c from the mitochondrial intermembrane space (IMS) to the cytosol where it binds protease-activating factor 1 (APAF1). Thereby, forming a structure termed the apoptosome that recruits and activates effector caspases such as caspase 9 which cleave and activate downstream caspases, caspase 3 and 7, that participate in the execution of apoptosis.<sup>37,39</sup>

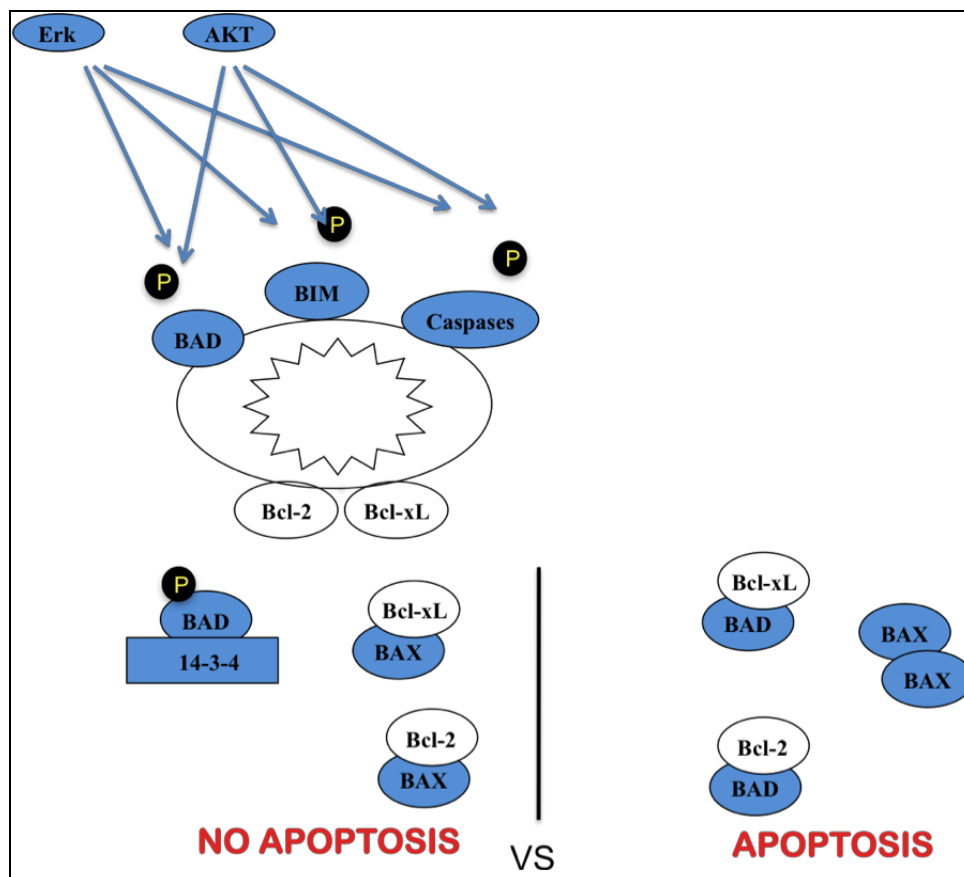


**Figure 7:** Interaction with Bad in the unphosphorylated state associates with Bcl-2 or Bcl-XL to promote apoptosis. Akt and ERK phosphorylates Bad on S136 and S112 respectively. These phosphorylation events cause Bad to associate with 14-3-3 proteins, thus inhibiting apoptosis.

A second BH3-only protein Bim, which has a major role in the death of haematopoietic cells is also regulated by the two pathways. Akt can directly phosphorylate Bim at S87 to promote binding to 14-3-3 proteins and inhibit its proapoptotic activity. ERK phosphorylation of Bim on S69 can result in ubiquitination of Bim and subsequent proteosomal degradation. In contrast to BAD, Bim is also modulated at transcriptional level.<sup>40</sup> Reports indicate that the pathways can cooperatively regulate the gene expression of Bim via the transcription factor, Foxo-3a. AKT and SGK can phosphorylate FOXO3A at Thr32, Ser253 and Ser315. Similar to post-transcriptional level, the 14-3-3 proteins bind the phosphorylated sites and sequester FOXOs in the cytosol, thereby abrogating their ability to enter the nucleus and activate quiescent, apoptotic genes expression. ERK phosphorylates FOXO3A at Ser294, Ser344 and Ser425, which increases FOXO3A interaction with the E3-ubiquitin ligase MDM2, thereby directing proteasomal degradation of FOXO3a.<sup>38</sup>

The pathways also enhance the translation of several weak mRNA that are often involved in apoptosis for example, Mcl-1. Such proteins possess tertiary structures that are difficult to translate and require the assembly of a translation complex which attaches to the 5' UTR. The two pathways control the assembly of the eIF4E translation apparatus. ERK, p90 RSK1 and p70SK6 are a few intermediary molecules involved in the regulation of weak mRNA translation. In some cases, the two pathways will phosphorylate the same molecule in the translation complex such ribosomal protein S6 (rpS6).<sup>1, 40</sup>

Recently it has been shown that the Raf/MEK/ERK cascade can phosphorylate the terminal effector molecule, caspase 9 on residue T125 which contributes to the inactivation of this protein.<sup>41</sup> Interestingly, caspase 9 is also phosphorylated by the Akt. The significance of the caspase 9 phosphorylation by Akt is arguable, as this phosphorylation site is not evolutionally conserved. However, cumulatively Raf/MEK/ERK and PI3K/Akt pathways appear to engage in intimate crosstalk to regulate the survival status of dividing cells.

### **1.5 The Raf/MEK/ERK, the PI3K/Akt Pathways and Cell Cycle**

Cell cycle regulation is bi-modal requiring signal from both the Raf/MEK/ERK and the PI3K/Akt pathways.<sup>42</sup> In mammals, all cells with the exception of liver and muscle rely on these pathways throughout their lifetime, for both development, and maintenance and repair. In a normal cell, the cell cycle is an orderly progression through four distinct phases G<sub>0</sub>/ G<sub>1</sub>, S, M, G<sub>2</sub>. In the S (Synthesis) phase, the cell duplicates its DNA and in the M (Mitotic) phase, the DNA is distributed equally between the two daughter cells. These two phases are separated by the two gap phases G<sub>0</sub>/G<sub>1</sub> and G<sub>2</sub>.

To ensure coordination, there is a restriction point at G<sub>0</sub>/G<sub>1</sub> and two additional checkpoints at the G<sub>1</sub>/S and G<sub>2</sub>/M. The core proteins involved in the regulation of these checkpoints are the cyclins and the cyclins dependent kinases.<sup>42</sup> These cyclin/ cdk complexes are formed during the different phases. The concentration of the cyclins are regulated by signaling, while the Cdk concentration stays the same throughout the cell cycle and whilst their activity is regulated in response to changes in cyclin concentration.

Present evidence indicates that CDK 4 and CDK 6 associate mainly with cyclin D in the regulation of G<sub>1</sub>. CDK1 associate with cyclin B to regulate G<sub>2</sub>/M transition, while CDK 2 is involved in the regulation of the G<sub>1</sub>/S transition and DNA synthesis by its association with cyclin E and cyclin A (Figure 8).<sup>43</sup> Cyclin D is one of its most cited transcriptional targets of the relevant to cell cycle, a major requirement for passage through the G<sub>1</sub> restriction point and commitment to the cell cycle. Sufficient accumulation of Myc is necessary for the activation of Cyclin

D expression, which subsequently associate with cyclin dependent kinases, phosphorylate Rb, release E2F and promote DNA synthesis.<sup>42,44</sup>

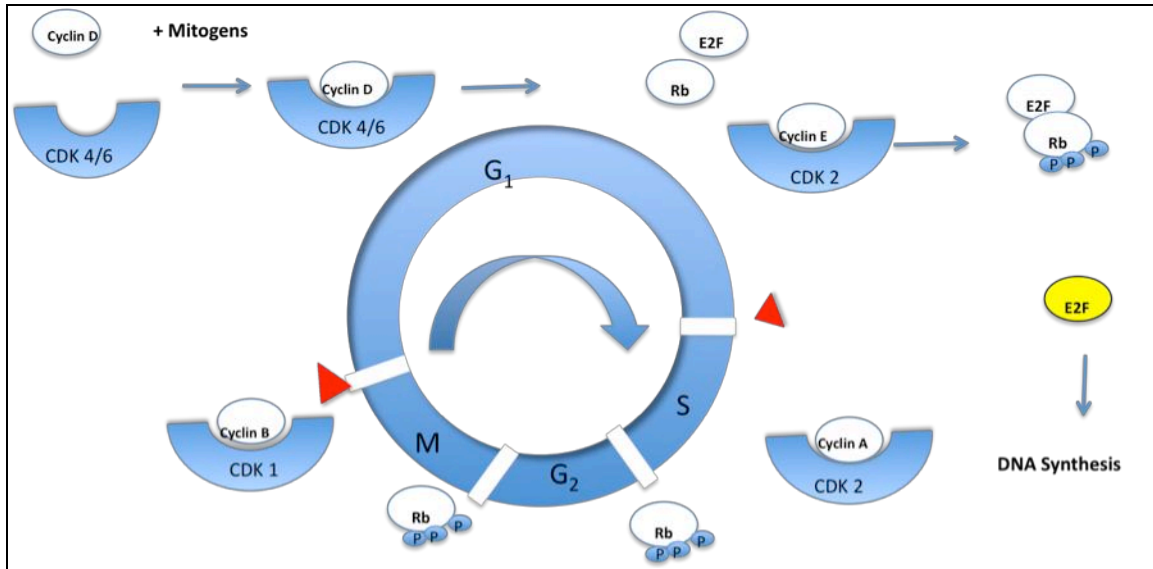


**Figure 8:** Erk and Akt stimulate cyclin D expression, and the association of cyclin D with CDK causes phosphorylation of Rb. In the phosphorylated state Rb release the E2F transcription factor promote DNA synthesis and progression through the phases.

The dynamic control of Myc by sequential phosphorylation allows Myc to integrate upstream signals from Erk and AKT. It can be substantially stabilized when phosphorylated at Ser62 by Erk activity. Subsequent phosphorylation of Myc at Thr58 by Gsk3, however, initiates a destabilization process in a sequential manner. Interestingly, phosphorylation at Thr58 requires prior phosphorylation at Ser62.<sup>38, 42, 45</sup> Hence, as Ras activity declines, Gsk3b cease the opportunity to initiates phosphorylation of Myc at Thr58 and triggers degradation.

By inactivating GSK-B, PI3K pathway blocks Myc degradation. There has been report of the pathways cooperatively increases cyclin D mRNA levels

increase of up to 20 fold, which generally peaks after 6 hours of mitogen stimulation.<sup>45</sup> In addition to inducing the transcriptional activation of cyclin D1 and D2, Ras signaling also stimulates the phosphatase Cdc25A that removes the negative regulatory phosphates from the Cdk. The myc transcription factor functions as a heterodimer with its obligate counterpart Max. The related protein Mad1 competes with Max. The myc/ max heterodimer positively regulates transcription whereas the myc/ mad1 represses transcription. Studies also indicate convergence of both pathways via RSK and S6K phosphorylate Mad1 on Ser 145. Thus, promoting Mad1 degradation, myc/max dimerization and induction of growth genes not exclusive to cyclin D.<sup>46</sup>

Careful dissection has revealed that while sustained ERK1/2 activation is required until the late G1 phase for successful entry into the S-phase, the accumulation of PI3K products is necessary for the late G1 progression.<sup>9</sup> Evidence shows that the stimulation of quiescent cells (Go) cause two peaks of activation. The first peak due to Raf/ MEK/ ERK activation and subsequent entry into the G1, and the second at mid-G1 phase the PI3K pathway peak. Several studies also suggest activation of the pathways in late S that persist until the end of mitosis. Present evidence indicates that their mechanisms of regulation differ during G<sub>2</sub>/M checkpoint. The inhibition of the PI3K pathway interferes with mitotic entry by cdc25 activation and increases cyclin B1 expression, whereas inhibiting the ERK pathway interferes with mitotic entry but has little effect on cdc25 activation and cyclin B1.<sup>47</sup>

## **1.6 Signaling Dynamics**

The Raf/MEK/ERK and PI3K/Akt pathways are driven by phosphorylation and de-phosphorylation reactions mediated by specific kinases, phosphatases, adaptor proteins and scaffolding proteins. The balance between these signals may widely vary in different tumors, and are important for sensitivity and outcome of drug therapy. However, the protein kinases have rapidly become one of the most pursued protein sub-family in the quest for novel drugs. Several compounds have been credited with putative chemotherapeutic activity. The majority of these inhibitors target various conformations of ATP, which often result in compounds exhibiting multiple kinase targets. Besides, in 2001 Imatinib (Gleevec) became the first therapeutic agent of a target molecule to enter clinical use. Imatinib acts by blockade of the non-receptor tyrosine protein kinase BCR-ABL.<sup>48,49</sup> Aberrant signaling by these chimeric proteins is rather similar to signaling activated by membrane bound receptor tyrosine kinase (RTK). The success of Gleevec has been the long-standing proof of concept for targeting the Raf/MEK/ERK and the PI3K/ Akt pathways.

The intrinsic mutations featured in the Raf/MEK/ERK are principally at Ras and Raf.<sup>14</sup> While several inhibitors have been developed to intercept oncogenic signaling, the Raf and MEK inhibitors remain the most attractive target of the Raf/ MEK/ ERK pathway. To date, pluripotent Raf inhibitor, Sorafenib (BAY43-9006) and the allosteric and highly selective MEK1/2 inhibitors, Sulumetenib (AZD6244) and PD0325901 are the best explored inhibitors of the Raf/MEK/ERK pathway. Sorafenib targets Raf, PDGFR and VEGFR, and was approved for the treatment



of advanced renal cancer.<sup>50,51</sup> CI-1040, the first MEK inhibitor to enter clinical trials, and its second generation inhibitors PD0325901 were well tolerated by patients but showed insufficient anti-tumor activity to warrant further development. Similarly, a second MEK inhibitor AZD6244 was terminated as a mono-therapy drug candidate in late phase trials in patients with melanoma, and it is currently in clinical trials for combination therapy.<sup>52</sup>

As for the PI3K/Akt pathway, mutations are most frequently reported at Akt, PTEN and PI3K. Within the PI3K/PTEN/Akt pathway, the main therapeutic targets: PI3K, mTOR and Akt (also referred to as PKB). In the PI3K pathway the second generation rapamycin analogs with improved pharmacological properties show productive therapeutic outcomes. The best evidence is the treatment of advanced renal cancer with temsirolimus, a rapamycin prodrug that has been FDA approved.<sup>53</sup> Others include the water soluble rapamycin (CCI-779) in phase III of development, and the two other agents, (RAD001) and (AP23573) in earlier phases of development. The PI3K inhibitors have been less successful. LY294002 and wortmannin, two well-known PI3K inhibitors, were shown to have effective anti-tumor activity, but had limited clinical value due to poor pharmacokinetic properties.<sup>54</sup> Likewise, perifosine, the most developed AKT inhibitor has not been shown to be beneficial as a single agent in several phase II studies.<sup>55</sup> Regardless, the repertoire of well-characterized inhibitors should not be discounted based on grim rate of success, as they have contributed a wealth of information to targeted cancer research.

While the small molecules inhibitors of the pathways are forecasted to

significantly impact the cancer chemotherapy, the underlying biochemical complexity remains a challenge. There exist several different layers of regulation which is heavily dependent on cell type, dosage and duration. Supporting studies indicate distinct differences in cell lines from same target tissue, although results from some *in-vitro* reports suggest similar mechanism from cell of differing origin. In a study by Kiyatkin this phenomenon was highlighted with MCF7 and T47D breast cancer cell lines. The T47D breast cancer cells displayed MEK resistance due to a PI3K/ AKT sensitive compensatory pathway, which was absent in the MCF7 breast cancer cell line which appear to signal predominantly through the MAPK pathway.<sup>56</sup>

There are also examples of dependence on dose and duration. In an elegant study by Haugh, ERK and PI3K -dependet Akt phosphorylation in PDGF-stimulated NIH 3T3 fibroblasts were evaluated using different combinations of ligand dose and stimulation time. The results supported the notion that the extent of ERK inhibition depends strongly on both dose and duration. At short stimulation time, ERK activation was substantially effected by PI3K inhibition when stimulated by low but not high PDGF concentration. The effect of Ras inhibition was similar but ERK phosphorylation was less sensitive to PDGF concentration.<sup>57</sup> The observed stimulation conditions are believed to be subject to negative feedback loops, but a definitive pattern is yet to emerge.

## 2. Crosstalk of the Raf/MEK/ERK and PI3K/Akt Signaling Pathways

The crosstalk between the two pathways is undisputed, and suggest high intimacy between the regulation of cell cycle and apoptosis (Figure 9). The transcription factors, Myc and E2F exist at the core of this interface. Myc activates E2F which promotes the transition of phase G1 to S the cell cycle. <sup>58</sup>Overexpression of E2F stimulates the expression of tumor suppressor, ARF, which inhibits the activity of MDM2. It is believed that the MDM2, an E3 ubiquitin ligase, targets p53 and accelerates its proteolytic degradation and maintains p53 at a low level. <sup>43</sup> Thus, by inhibiting MDM2, ARF prevents p53 degradation and consequent stabilization. This would result in either p53 dependent apoptosis or cell cycle arrest due to p53 blockade.

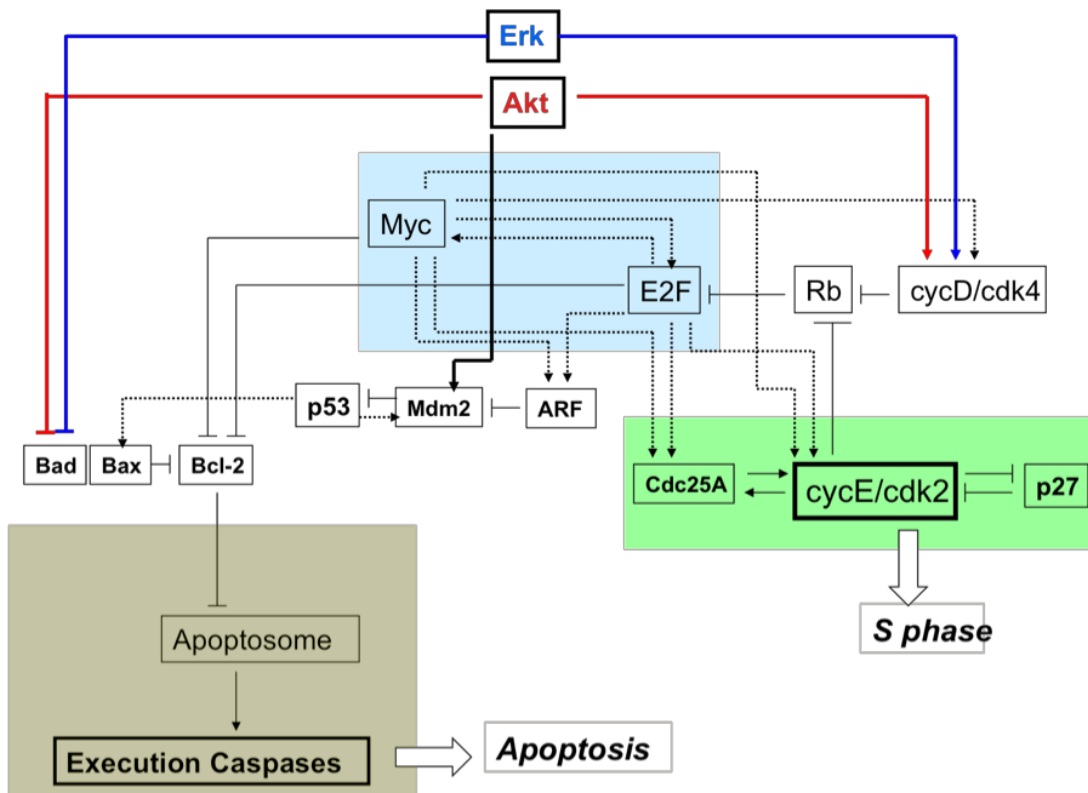


**Figure 9.** Simplified representation of the crosstalk between Erk and Akt; and the cell cycle and apoptosis.

A direct consequence of the crosstalk is the generally disappointing single-targeted therapy against the different components developed based on traditional understanding of the means by which these pathways were thought to govern cell processes. The pathways were characterized as simple, linear and unidirectional. However, emerging studies have revealed that the two seldom act in isolation, but rather through multiple crosstalk and feedback interaction within a complex, well-coordinated network (Figure10).<sup>38</sup> As such, it is apparent that perturbations targeting specific signaling molecules may have unexpected effects, and in some cases the compensatory pathways have been shown to mediate drug resistance.<sup>59</sup> In view of this, a great deal of effort has been focused on experiments aimed at improving the understanding of the interplay and molecular mechanisms of the two pathways, which will in turn provides access to novel strategies with improved clinical outcome.

Encouragingly, several studies indicate that simultaneous inhibition of the pathways may be required for optimal efficacy. Theoretically, the complete blockage of the pathways at upstream receptors may be valid, but could have deleterious effects and may result in significant normal cell toxicity. Alternatively, blocking a subset of downstream effector molecules would be a more pragmatic approach. Interestingly, there have been collaborations between large pharmaceutical companies. For example, the combination of Novartis' PI3K inhibitor (BKM120) and GSK's MEK inhibitor (GSK1120212) in phase I development for triple negative breast cancer. Similarly, the combination of AstraZeneca's MEK inhibitor (AZD6244) and Merck's Akt inhibitor (MK2206)

undergoing phase I trials for locally advanced or metastatic solid tumors.<sup>26</sup> Evidently, a single compound targeting both pathways is a realistic therapeutic option with inherent advantages of increased patient compliance and reduced risk of drug resistance.

### **3. Rationale: Discovery and identification of lead dual-pathway inhibitor of the Raf/MEK/ERK and PI3K/AKT signaling pathways.**

**3.1 Development of ERK1/2 inhibitor.** ERK1/2 represents a near optimal target to develop such inhibitors given the following facts: (1) the important position of ERK1/2 in the Raf/MEK/ERK1/2 pathway that controls the distribution of signals from upstream; (2) the disclosure of the crystal structures of ERK2; and (3) The identification of the docking groove composed of a common docking (CD) domain and an ED domain on ERK2 and the validation of their roles in the control of docking interaction with substrate proteins. Taking advantage of a favorable situation, the Shapiro's group identified several such inhibitors by computer-aided virtual screening of a small library of compounds (Fig. 10).<sup>60</sup>

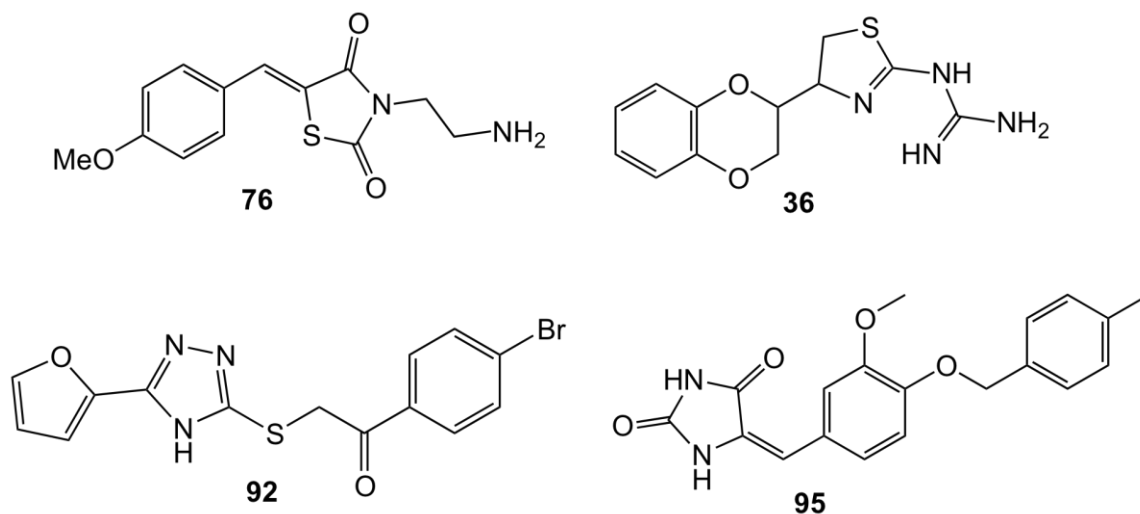


**Figure 10:** Putative substrate-specific ERK 1/ 2 inhibitors

Among these structures, compound 76 represents an interesting chemical scaffold. Compound 76 inhibited the phosphorylation of the downstream substrate of ERK1/2, Rsk and Elk-1, in U937 cells with minimal effects on the phosphorylation of ERK1/2. In addition, small molecules containing the

thiazolidine-2,4-dione moiety, such as the anti-diabetic drug troglitazone, have been recently reported to have anti-cancer activities. Thus, these results demonstrated the potential of compound 76 as a new chemotype to develop substrate-specific ERK1/2 inhibitors.<sup>60</sup>

Due to the fact that compound 76 was discovered as a lead through screening, little information about the pharmacophore of compound 76 is known and there have been no reports of efforts to modify 76 to improve its bioactivity. In a previous study, we initiated preliminary structure-activity relationship (SAR) studies of compound 76 to define its pharmacophore and to search for more potent and selective substrate-specific ERK1/2 inhibitors. Immunoblot studies established that 1c showed improved activity compared to 76 (Fig. 13A).<sup>61</sup>

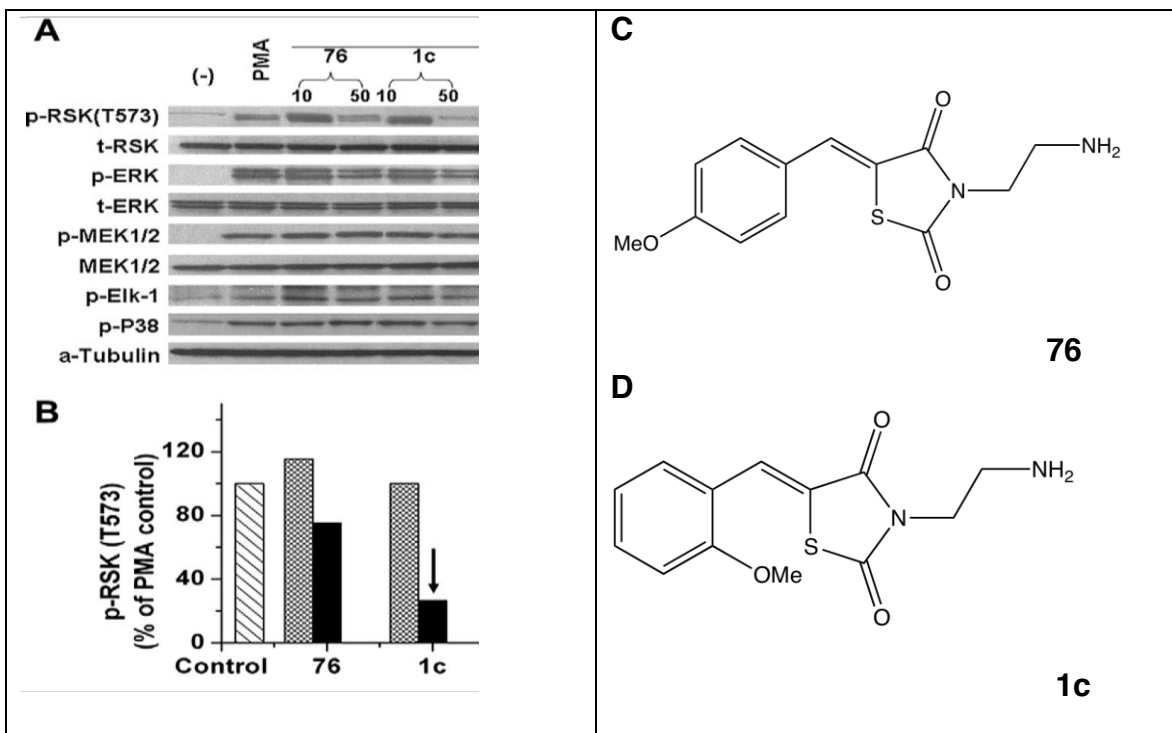


**Figure 13:** Effect of test compound on Rsk, ERK 1/2, Elk-1, MEK 1/2 and p38 phosphorylation. A: Immunoblot results B: Quantification of Rsk-1 phosphorylation by densitometry C: Compound 76 and D: Compound 1c.

**3.2 Discovery of a lead dual-pathway inhibitor.** In our effort to design and discover novel templates targeting the Raf/MEK/ERK and the PI3K/AKT signaling cascade, we have embarked on further characterization of our recently discovered lead ERK inhibitor, 1c. Preliminary structure–activity relationship (SAR) studies was initiated to define its pharmacophore. To facilitate the structure activity relationship the lead was again divided into three domains: a phenyl ring domain, a thiazolidinedione domain and an ethylamine domain. Compound 1 emerged as a novel chemotype with several features that may have contributed to its activity. These include the phenylpropylidene double bond as a Michael addition acceptor, the primary amine for ionic interaction and the aromatic ring for hydrophobic interaction.<sup>63</sup>

The cell viability and proliferation effect of compound 1 was investigated using the [(3- (4,5-dimethylthiazol-2-yl)-5-(3-carboxymethoxyphenyl)-2-(4-sul-fophenyl)-2H-tetrazolium] (MTS) assay and <sup>3</sup>H thymidine respectively in U937 cells. The known MEK inhibitor PD184352 was used as positive control. Compound 1 exhibited significant inhibition on U937 cell viability at higher concentrations (15, 20, and 25  $\mu$ M) but not at concentration less than 10  $\mu$ M (Figure 13C). Since the MTS assay only examines the metabolically healthy cells, but cannot distinguish whether the cells are actively dividing or quiescent, the [3H]- thymidine incorporation assay was used to investigate the actively dividing cells by detection of DNA synthesis. At 10  $\mu$ M, 1 significantly inhibited the [<sup>3</sup>H]-thymidine incorporation, while PD184352 did not. At 30  $\mu$ M, 1 almost completely inhibited [<sup>3</sup>H]-thymidine incorporation, and PD184352 also exhibited



significant inhibition at this concentration (Figure 13D). Taken together, these results may indicate that 1 may induce early apoptosis of U937 cells through inhibiting DNA synthesis at 10  $\mu$ M but not affecting cell viability.

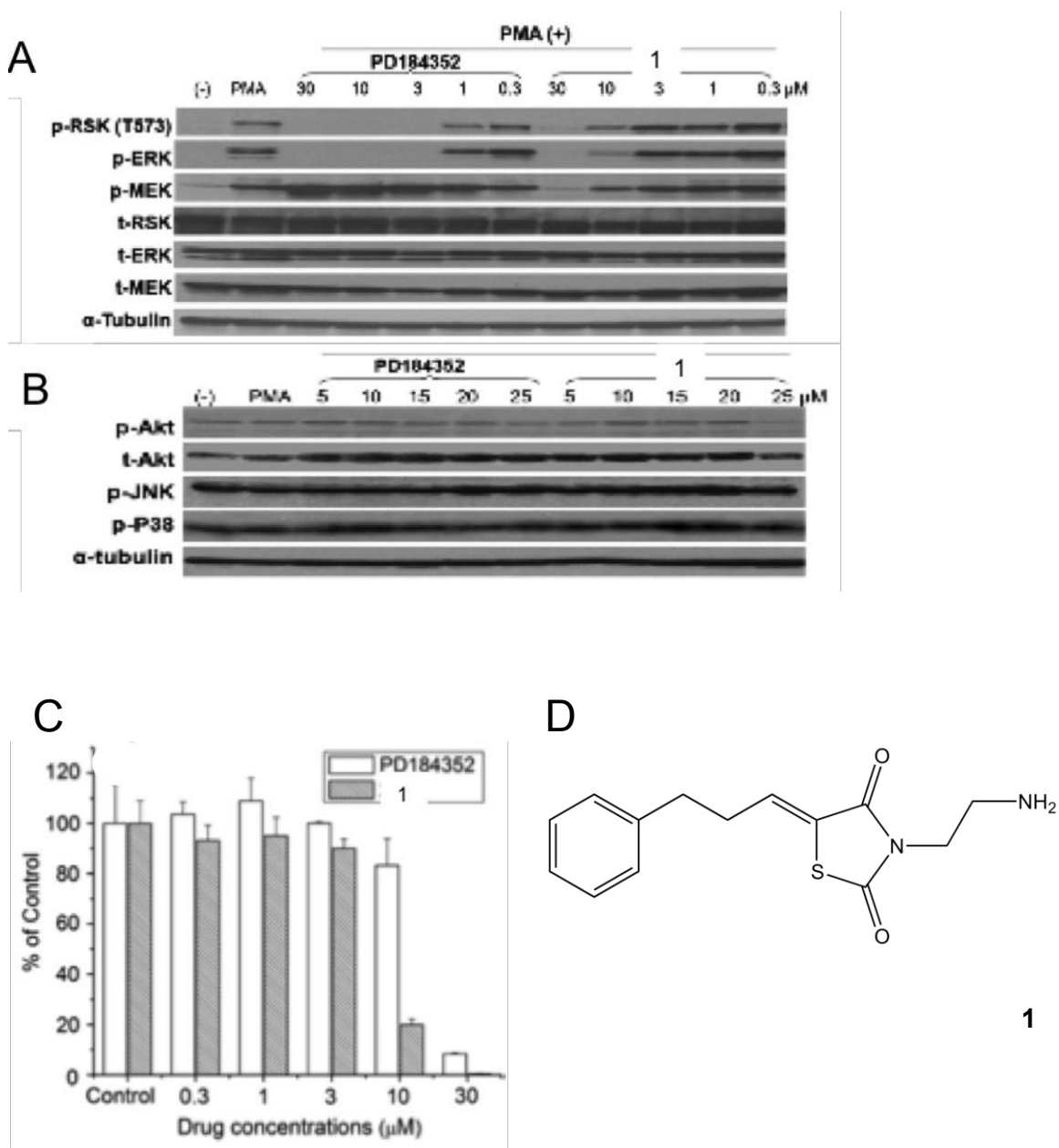


**Figure 14.** Western blot analysis of compound 1 and its analogs in U937 cells a) Raf/MEK/ ERK components b) PI3K components. Inhibition of cell proliferation using MTS assay (c) and [3H]-thymidine incorporation (d) in human leukemia U937 cells.

To get insight into the signaling pathways that are possibly involved in 1's

functional activities, Western blot analysis was then performed in U937 cells. As shown in Figure 14A, PD184352 significantly inhibited the phosphorylation of both ERK and its downstream substrate Rsk1 at as low as 3 $\mu$ M concentration. Compound 1 also significantly inhibited the phosphorylation of ERK and Rsk1 at 10  $\mu$ M and 30  $\mu$ M concentrations, therefore being slightly less potent than PD184352 (Figure 14). However, when the p-MEK level was evaluated, it is notable that 1 induced dose dependent decrease the p-MEK level in U937 cells while treatment with PD184352 resulted in a dose-dependent increase in the p-MEK levels, which is consistent with the reported negative feedback mechanism in the Raf/MEK/ERK pathway. Interestingly, 1 at 25  $\mu$ M significantly suppressed p-Akt levels while the specific MEK inhibitor showed no inhibitory effects. This might indicate that 1 targets either an upstream activator of MEK in the Raf/MEK/ERK signaling pathway or it inhibits MEK via a different mechanism.

**4. Objective: Development of oxindole analogs as potential dual pathway inhibitors and anticancer agents.** In order to develop novel chemotype of dual-pathway inhibitors as well as to develop a chemical template that would provide more flexibility for future structural modification, we intend to replace the TZD ring with an oxindole ring (Figure 15). The oxindole was identified as a more attractive replacement for the thiazolidinedione ring based on parallel study with the maleimide analog using the MTT assay. The design hypothesis was that both ring system would orient the critical structural features such as the ring system, the spacer and the ethylamine tail in a similar manner to that in the TZD analogs, and thereby retain the biological activity as dual-pathway inhibitors of the Raf/MEK/ERK and PI3K/Akt signaling pathways.

In comparison to the thiazolidinedione lead, the oxindole analog showed improved potency (4-fold increase) while the maleimide analog showed a decrease in potency (10-fold decrease). This suggests that the aromatic ring system of the oxindole ring which is absent in the maleimide ring may contribute to the observed activity. The results were also consistent with the recognition of the oxindole template as a privileged template in drug discovery. In addition to the oxindole analog being 4-fold more potent than the lead compound 1, the oxindole ring would also provide greater flexibility to allow the introduction of various substituents, and thus facilitate comprehensive SAR studies for future investigation.

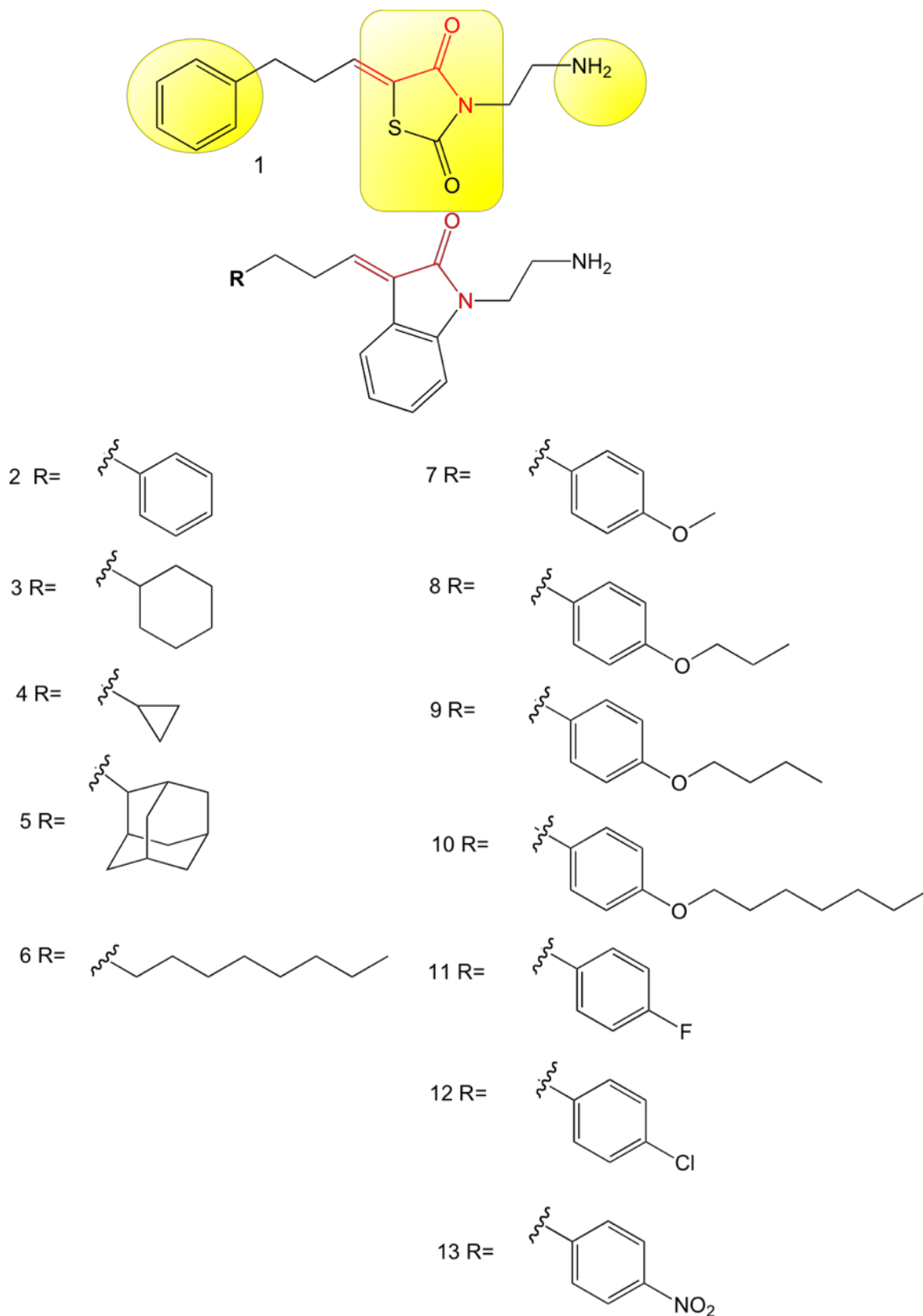
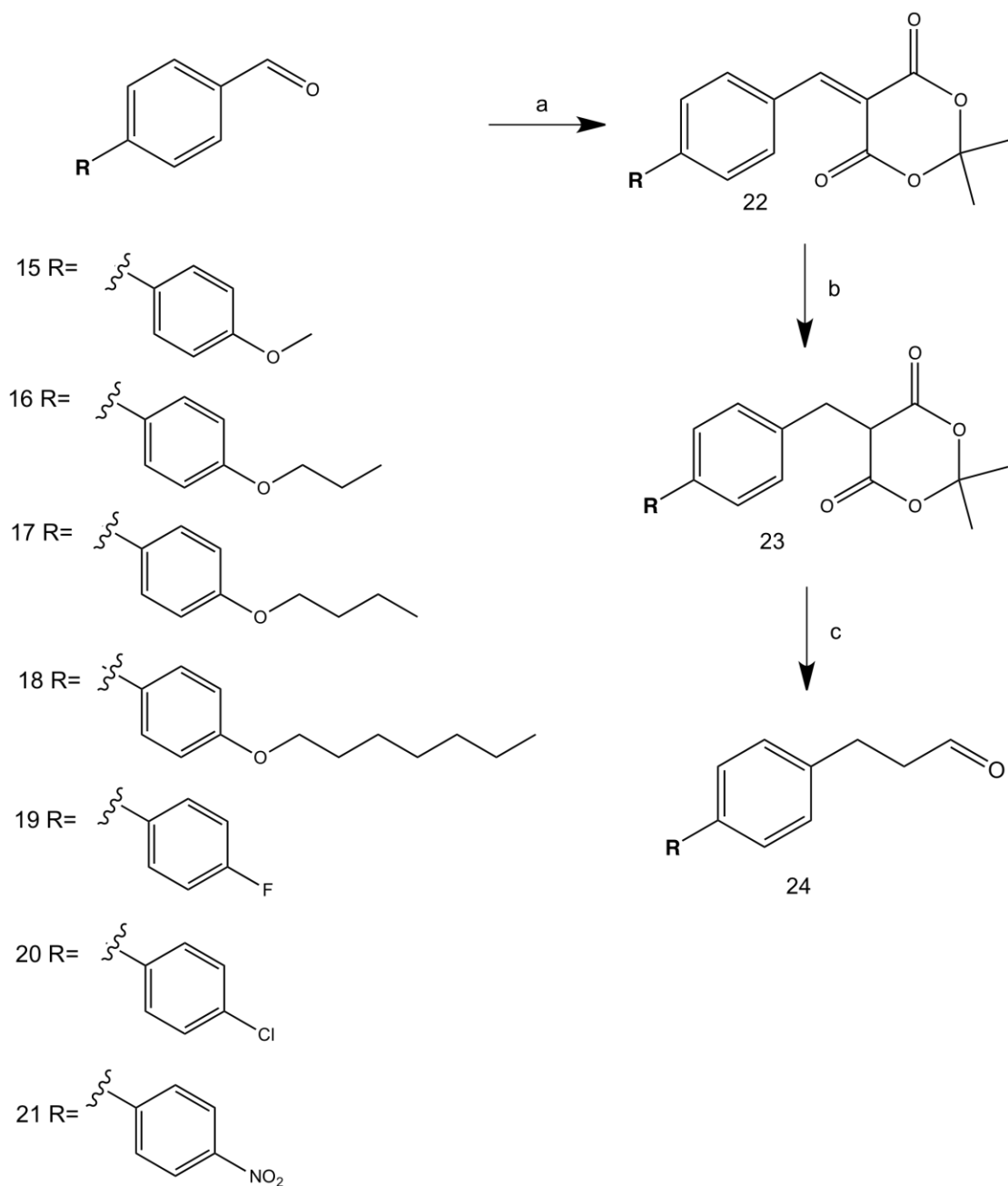


**Figure 15:** Thiazolidinedione lead and designed oxindole analogs.

**4.1 Design of oxindole analogues.** To obtain structural information about the features of compound 2 that are critical to the anticancer activity, compound 2 was divided into the said three domains like compound 1, namely (1) phenyl ring domain; (2) ethylamine domain and (3) oxindole domain. As shown in figure 15, compounds 2-6 were designed to highlight the role of the aromatic ring in biological activity. Particularly, it was examined if the replacement of the phenyl ring with cyclohexyl, adamantyl, cyclopropyl or nonyl groups would be tolerated or improve activity. Compounds 7-13 were designed to evaluate the influence of electrostatic and sterics of the substituent on the phenyl ring on the biological activity. The substitutions were made in 4-phenyl position and varied from high to moderate electron-donating and electron-withdrawing groups (Figure 15).

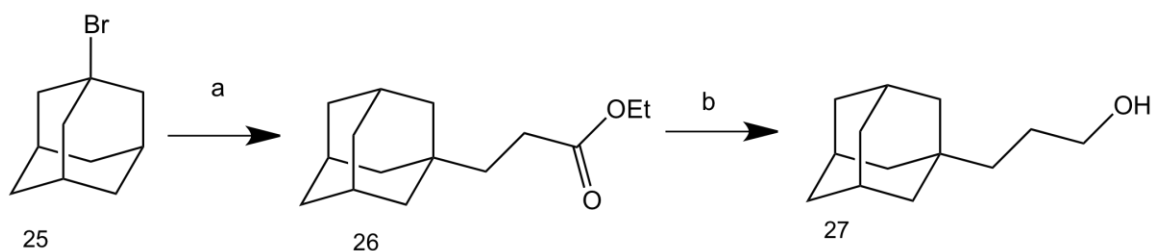
The synthesis was initiated with the preparation of various aldehydes as shown in Scheme 1. The substituted benzaldehydes were converted to their Meldrum's acid derivatives followed by reduction and hydrosilylation to give the different aldehydes.



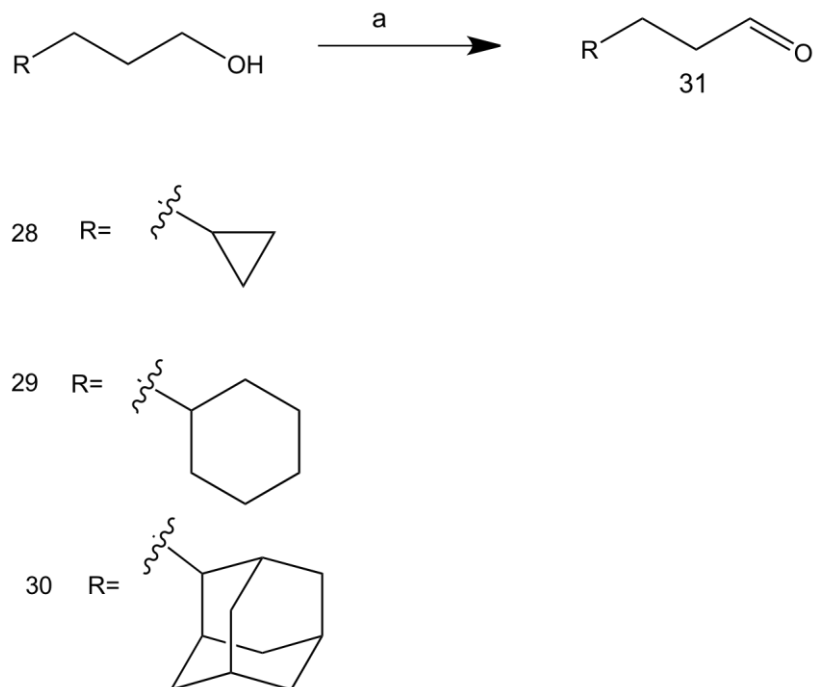
**Scheme 1:** a) Meldrum acid, piperidine, EtOH b) NaBH<sub>4</sub>, AcOH, CH<sub>2</sub>Cl<sub>2</sub>; c). PhSiH<sub>3</sub>, Et<sub>3</sub>N, THF c) DMSO, (COCl)<sub>2</sub>, Et<sub>3</sub>N, CH<sub>2</sub>Cl<sub>2</sub>, -78°C

The synthesis 3-cyclohexylpropanal, 3-cyclopropylpropanal as well as 3-adamantan-1-yl)propanal was achieved through the oxidation. While (3-cyclohexylpropanal and 3-cyclopropylpropanol were commercial available, 3-

adamantan-1-yl)propanal required synthesis. As shown in scheme 2, this synthesis started with the radical conjugate addition of bromoadamantane 25 to ethyl acrylate using  $n\text{Bu}_3\text{SnH}$  to afford the adamantyl ester 26. Reduction with lithium aluminum hydride (LAH) then yielded the primary alcohol 27. 3-cyclohexylpropanol, 3-cyclopropylpropanol as well as 3-adamantan-1-yl)propanol were subsequently obtained by swern oxidation



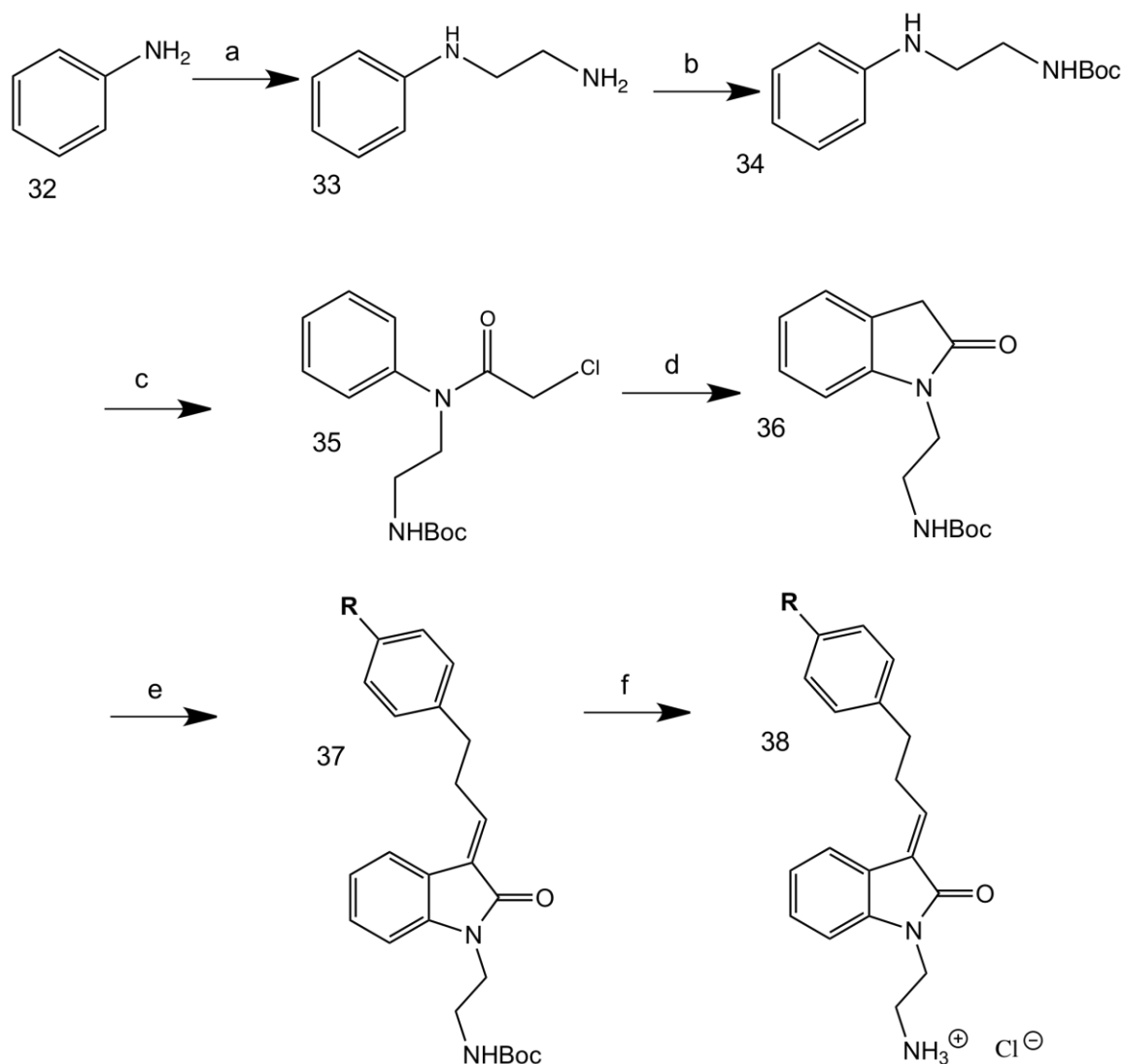
**Scheme 2:** a)  $n\text{Bu}_3\text{SnH}$ , AIBN, ethyl acrylate, toluene, rt b) LAH, THF, rt c) DMSO,  $\text{ClCH}_2\text{OCl}$ ,  $\text{Et}_3\text{N}$ ,  $\text{CH}_2\text{Cl}_2$ ,  $-78^\circ\text{C}$



**Scheme 3:** a) DMSO,  $\text{ClCH}_2\text{OCl}$ ,  $\text{Et}_3\text{N}$ ,  $\text{CH}_2\text{Cl}_2$ ,  $-78^\circ\text{C}$

In retrospect, compound 36 was synthesized in a four-step reaction beginning with aniline. The N-substituted Boc analog of aniline was synthesized from the alkylation reactions with 2-bromoethylamine and carbamic acid tert-butyl ester. The secondary amine of compound of compound 34 was readily acetylated to the chloroacetanilide. With catalytic amounts of palladium acetate in combination with 2-(di-tert-butylphosphino)biphenyl as a ligand, and triethylamine as base, the chloroacetanilides was converted to oxindoles with high levels of regioselectivity. Knoevenagel condensation of the various aldehyde with compound 36, followed by the removal of Boc or tert-butyl ester group afforded compounds 2-13 (scheme 4).



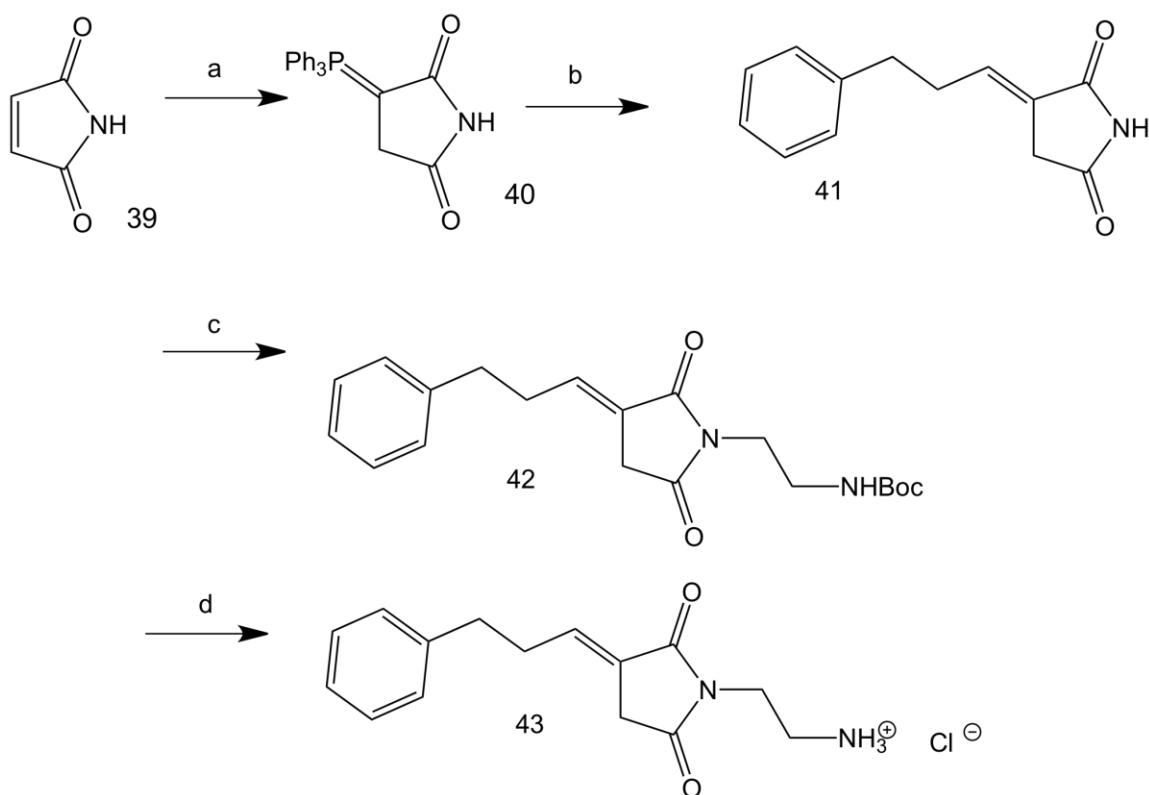


**Scheme 4:** a)  $\text{H}_2\text{NCH}_2\text{CH}_2\text{Br}$ , toluene, reflux; b)  $\text{Boc}_2\text{O}$ , MeOH, rt c)  $\text{ClCH}_2\text{OCl}$ ,  $\text{CH}_2\text{Cl}_2$ ,  $0^\circ\text{C}$ , d)  $\text{Pd}(\text{OAc})_2$ , L,  $\text{Et}_3\text{N}$ , toluene,  $80^\circ\text{C}$  e)  $\text{RCHO}$ , piperidine, EtOH, reflux (f) Dioxane-HCl, EtOAc

The scheme employed to synthesized the oxindole analogues was carefully devised. As a starting material, aniline has the advantage of being cheap and available. Another favorable feature of this synthetic route is the palladium catalyzed C-H functionalization. This step circumvent the need for high temperature as in the Wolff-Kishner reduction of isatin to oxindole, as well as the

combination of both high temperature and strongly acidic in Friedel-Craft reaction. Abrogating the need for harsh conditions, the palladium-catalysed synthesis of oxindole cyclization is highly compatible extending to even electron deficient aromatic systems.

The maleimide analog 43 in the preliminary set of experiment was also synthesized. The condensation of the maleimide and hydrocinnamaldehyde was achieved by Wittig reaction through a phosphorane intermediate 40. The N-alkylated product 42 was obtained by Mitsunobu reaction.



**Scheme 5:** (a)  $\text{PPh}_3$ , acetone, reflux; (b)  $\text{RCHO}$ , methanol, reflux; (c)  $\text{BocNHCH}_2\text{CH}_2\text{OH}$ ,  $\text{PPh}_3$ , DIAD; (d) Dioxane-HCl, EtOAc.

### **3. Discussion**

**3.1 Anti-proliferative activity in human leukemia U937 cells.** The activation of the Raf/MEK/ERK and PI3K/Akt signaling pathways has been shown to play multiple roles in the cell proliferation and apoptosis of hematopoietic cells including U937 cells. Accordingly, the U937 cells were employed for preliminary testing of the compounds. We first tested the anti-proliferative activity of the designed oxindole analogs. Notably, as shown in Table 1, all of the designed compounds exhibited anti-proliferative activity against the growth of U937 cells with micromolar or sub-micromolar potency. This also confirms that oxindole template can retain the anti-proliferative activity of these analogs, thus supporting our design rationale.

Compared to lead compound 1, compound 2 in the oxindole series improved anti-proliferation activity (4-fold increase). While the cyclohexyl analog exhibited improved antiproliferation activity in comparison to compound 2, in the oxindole series, compound 3 exhibited comparable effects to compound 2, suggesting that sterics may not play a pivotal role since the phenyl ring is planar whereas the cyclohexyl group can flip between the chair, boat and other translational conformations. This notion was further supported by the fact that 4 and 5 with the cyclopropyl ring and the adamantyl ring respectively showed comparable anti-proliferation potency with compound 2.

Compounds 7 and 8 exhibited anti-proliferative activity with sub micromolar potency, the best two among the compound tested here. Combining the results from compound 2-6, this may indicate that the target protein may contain

a narrow binding pocket to interact with phenyl group through hydrophobic interactions. This hypothesis was further supported by the results of compounds 9 and 10 with reduced potency in comparison to 7 and 8. As compound with electron-withdrawing substitutions on the phenyl ring (compounds 11-14) they also exhibited comparable potency to compound 2, suggesting mainly hydrophobic interactions with the phenyl ring. Interestingly, variation of the inhibitory effect on the U937 was most evident at 3  $\mu\text{M}$  of drug concentration, which is around the average  $\text{IC}_{50}$  value for the series (Figure 17). Notably, compound 7 was observed to significantly inhibit cell growth at 3  $\mu\text{M}$  (73.5 % inhibition) while other compounds achieved the same inhibition at 10  $\mu\text{M}$ .

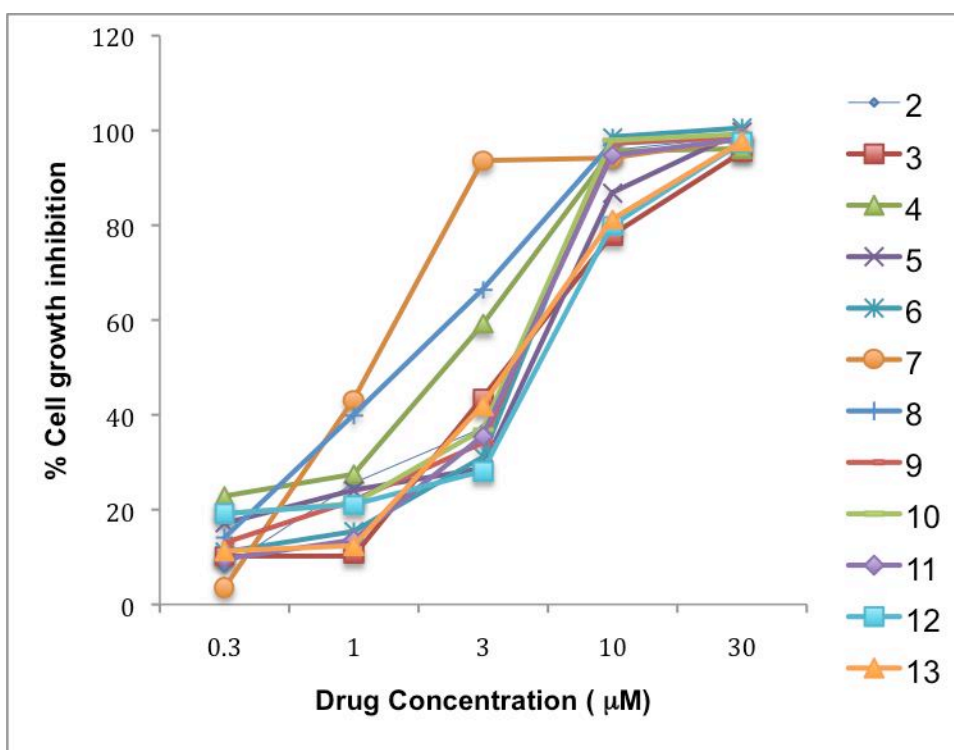


**Figure 16:** U937 cells were treated with compounds 2-13 for 72 hours and the viability was analysed using the MTT assay

Compound	IC50 ± SEM	Compound	IC50 ± SEM	Compound	IC50 ± SEM
2	2.128 ± 0.006	6	3.5 ± 0.3	10	3.9 ± 0.3
3	2.7 ± 0.2	7	0.92 ± 0.04	11	2.69 ± 0.06
4	1.16 ± 0.05	8	0.95 ± 0.11	12	4.0 ± 0.7
5	4 ± 1	9	4.6 ± 0.8	13	3.6 ± 0.2

**Table 1:** Growth inhibition of U937 cells by compounds 2-13 (μM)

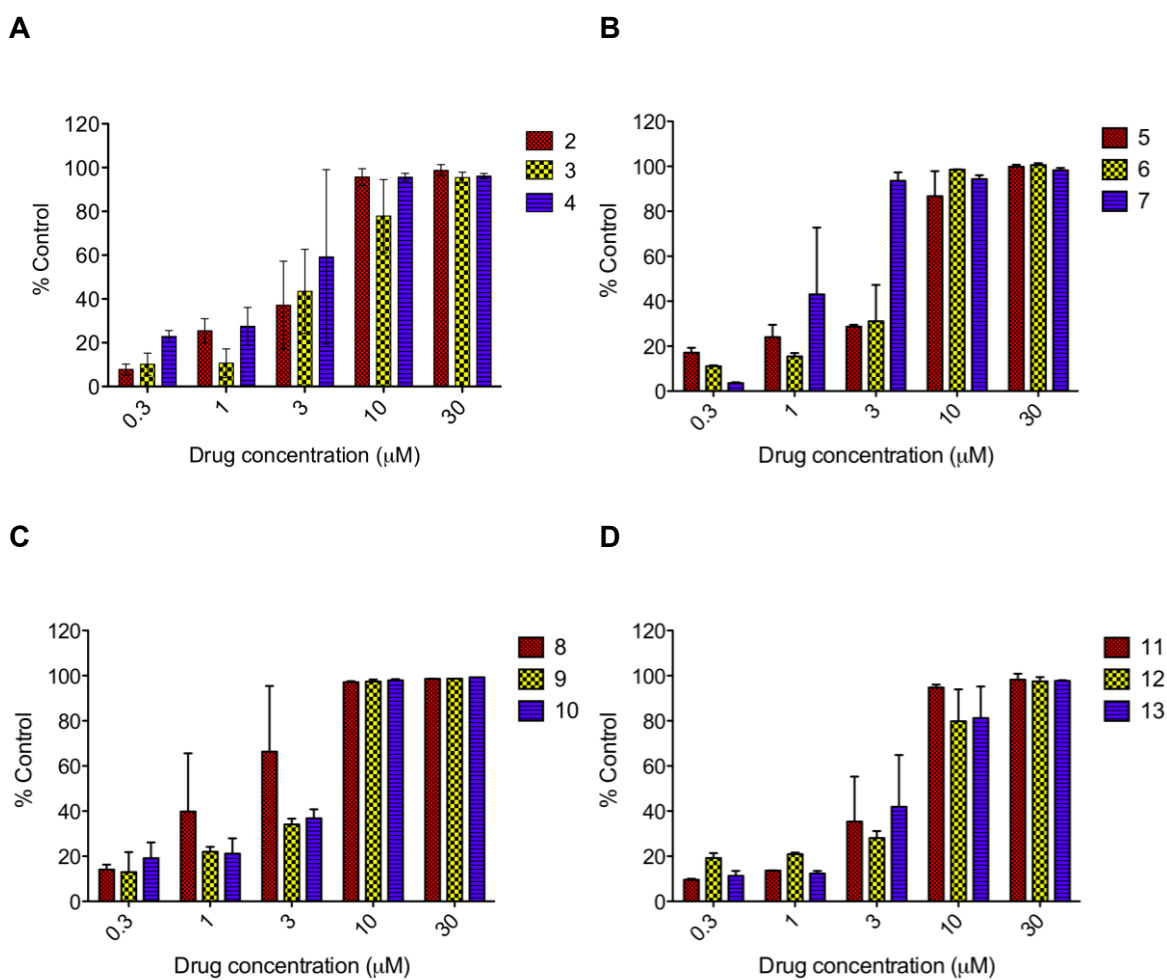


**Figure 17:** Anti-proliferative effects of compounds on U937 cells assayed using MTT.

**3.2 Western Blot Analysis of compounds 7 and 10.** To confirm that the growth inhibition of U937 cells by these oxindole analogs were mediated through the inhibition of the Raf/MEK/ERK and PI3K/Akt signaling cascades. Compounds 7 and 10 were selected for western blot analysis in U937 cells, as compound 7 was the most active one among the tested analogs and its comparison with compound 10 may shed some light on mechanistic information.

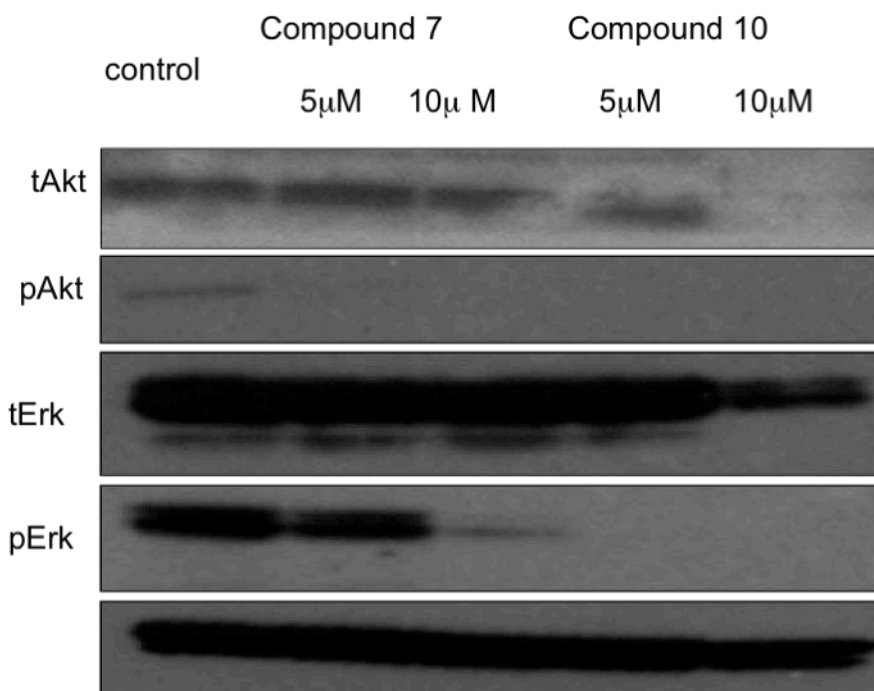


**Figure 18:** U937 cells were treated with Compound 7 and 10 at the indicated concentrations for 24 hours. Lysate from culture was analyzed by primary antibodies.

As shown in Figure 18, both compounds consistently suppressed the expression of the critical components of these two signaling pathways, p-ERK and p-AKT, at concentration as low as 5 μM. Surprisingly, compound 10 appeared to have a more significant effect on inhibition of p-ERK than compound 7, while compound 7 is more potent than compound 10 in the anti-proliferation

assay of U937 cells. This may indicate that a more balanced inhibition on both signaling pathway is necessary to show optimal pharmacological outcome. As reflected by anti-proliferation here, the significant inhibition of one signaling pathway does not equal to the optimal cytotoxic effects, thus, further attesting to the rationale of designing dual-pathway inhibitors. Taken together, the results of the anti-proliferative assay and western blot indicate that signaling blockage and growth inhibition by these newly designed oxindole analogs in U937 cells are correlated.

**3.3 Apoptotic effects of compounds 7 and 10.** As the Raf/MEK/ERK and PI3K/Akt signaling pathways have been demonstrated to play important roles in regulating apoptosis, the apoptotic effects of 7 and 10 were evaluated in U937 cells using cytometry to obtain preliminary mechanistic data for the anti-proliferative activity. As shown in Figure 19, both compounds significantly induced apoptotic effects on U937 cells after 24 hr treatment at as low as 5 M (63.9% and 21.7% for compound 7 and compound 10, respectively).

Both compounds also induced significant apoptosis at 10  $\mu$ M. Interestingly, compound 7 induced early apoptosis at both concentrations while compound 10 only induced late apoptotic effects in U937 cells under the experimental conditions. As discussed above, compound 7 and compound 10 have different inhibitory effects on the Raf/MEK/ERK and PI3K/Akt signaling pathways as demonstrated by western blot results. This phenomenon might contribute to the distinct apoptotic effects since both signaling pathways can

regulate apoptosis through differential downstream substrates. This also does not rule out the possibility of the involvement of other off-targets that these two compounds might interact. Further studies are needed to get more information about the mechanism underlying the different apoptotic effects in U937 cells.

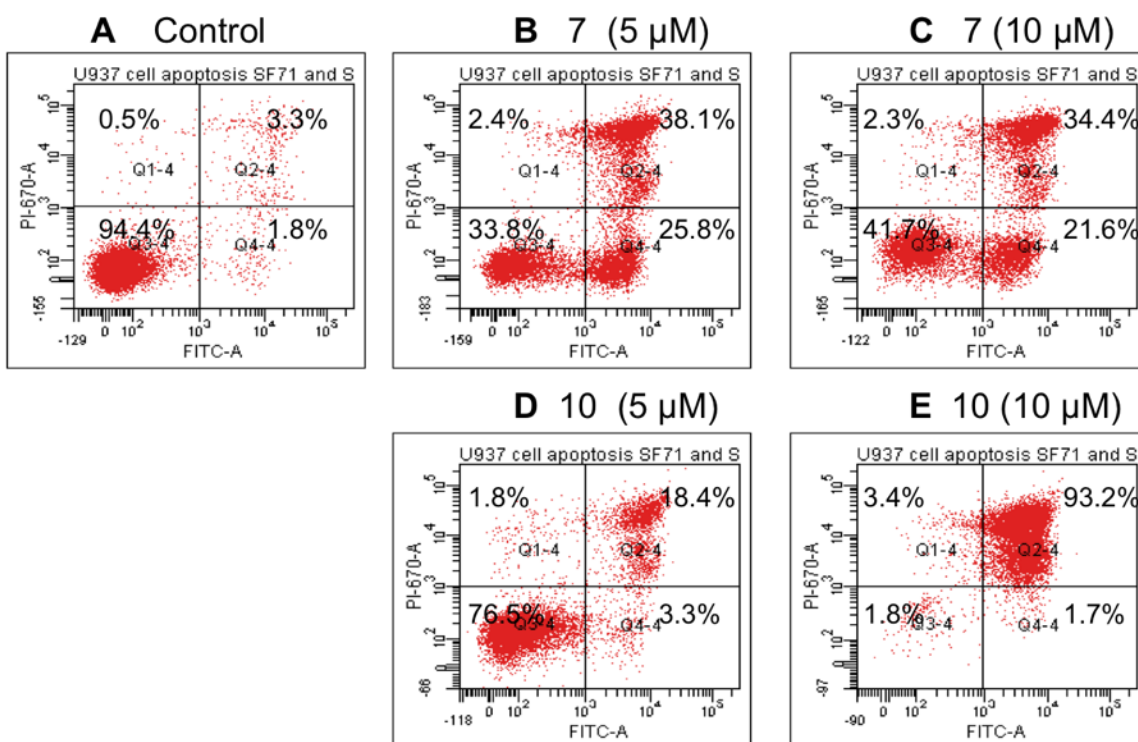


**Figure 19:** Compounds 7 and 10 induced apoptosis in U937 cells. The U937 cells were treated for 24 hours with the drugs, after which they were stained with Annexin VI/ PI and analyzed by flow cytometry.



**3.4 Conclusion** In summary, the work presents the design and biological characterization of a series of oxindole compounds as novel dual-pathway inhibitors of the Raf/MEK/ERK and PI3K/AKT pathways. The MTT anti-proliferative assay, western assay and apoptotic assay were employed to investigate biological activity in human leukemia U937 cells. All of the designed compounds exhibited anti-proliferative activity against the growth of U937 cells with micromolar or sub-micromolar potency. Western blot analysis correlated the anti-proliferative activity of the Raf/MEK/ERK and PI3K/Akt signaling pathways with suppression of critical pathway components. Lastly, the apoptotic assay shed some light on the preliminary mechanistic information. Taken together the results strongly support our design rationale by showing anti-proliferation, inhibitory effects of the signaling pathways, and apoptotic effects of these oxindole analogs. The results also suggest the potential of the oxindole template as new lead compounds to develop newer generation of dual-pathway inhibitors of the Raf/MEK/ERK and PI3K/Akt.

## 5. Experimental

General Procedure for Preparation of meldrum's acid intermediates: To a solution of Meldrum's acid (1.2 mmol) and 5 drops of piperidine in ethanol aryl aldehyde was added. The resulting solution was stirred at room temperature overnight. The reaction mixture was filtered via Buckner filtration and washed with ethanol and methanol to obtain the pure intermediate.

### **5-(3-(4-Methoxyphenyl)-methylene)-2,2-dimethyl-1,3-dioxane- 4,6-dione (15)**

<sup>1</sup>H NMR (300 MHz, CDCl<sub>3</sub>): 8.38 (s, 1H), 8.24-8.21 (d, J = 9.3 Hz, 2H), 6.99-6.97 (d, J = 9.3 Hz, 2H), 3.91 (s, 3H), 1.79 (s, 6H).

### **5-(3-(4-Ethoxyphenyl)-methylene)-2,2-dimethyl-1,3-dioxane- 4,6-dione (16)**

<sup>1</sup>H NMR (300 MHz, CDCl<sub>3</sub>): 8.37 (s, 1H), 8.23 (d, J = 9.3 Hz, 2H), 6.97-6.99-6.55 (d, J = 9.3 Hz, 2H), 4.13-4.08 (q, J = 7.0 Hz, 2H), 1.78 (s, 6H), 1.26-1.23, (t, J=6.9Hz, 3H).

### **5-(3-(4-Butoxyphenyl)-methylene)-2,2-dimethyl-1,3-dioxane- 4,6-dione (17)**

<sup>1</sup>H NMR (300 MHz, CDCl<sub>3</sub>): 8.37 (s, 1H), 8.22-8.21 (d, J = 9.3 Hz, 2H), 6.97-6.95 (d, J = 9.3 Hz, 2H), 4.09-4.06 (q, J = 7.0 Hz, 2H), 1.78 (s, 6H), 1.55-1.45 (m, 2H), 1.01-0.97 (t, J=7.4 Hz, 3H)

### **5-(3-(4-Chlorophenyl)-methylene)-2,2-dimethyl-1,3- dioxane-4,6-dione (19)**

<sup>1</sup>H NMR (400 MHz, CDCl<sub>3</sub>): d 8.37 (s, 1H), 8.04-8.02 (d, J = 8.7 Hz, 2H), 7.47-7.45 (d, J = 8.7 Hz, 2H), 1.81 (s, 6H).

### **5-(3-(4-Florophenyl)-methylene)-2,2-dimethyl-1,3- dioxane-4,6-dione (20)**

<sup>1</sup>H NMR (400 MHz, CDCl<sub>3</sub>): 8.39 (s, 1H), 8.19-8.15 (m, 2H), 7.17 (t, J=8.5 Hz, 2H), 1.80 (s, 6H)

### **5-(3-(4-Nitrophenyl)-methylene)-2,2-dimethyl-1,3-dioxane-4,6- dione (21)**

<sup>1</sup>H NMR (300 MHz, CDCl<sub>3</sub>): d 8.46 (s, 1H), 8.32-8.29 (d, J = 9.3 Hz, 2H), 8.08.08-8.05 (d, J = 9.3 Hz, 2H), 1.84 (s, 6H).

To a solution of 5-arylidene Meldrum's acid derivative (1 mmol) and glacial acetic acid (4 mL) in dichloromethane at 0°C was added sodium borohydride (3.2 mmol) dropwise. The solution was dissolved in dichloromethane and washed with brine and water. The organic phase was extracted, dried over NaSO<sub>4</sub>. The monoakyl meldrum acid derivative (1 mmol) was dissolved in THF. Triethylamine (2 mmol) was then added followed by phenysilane (3 mmol). The resulting solution was stirred for 2 hrs at room temperature. Water was added to the solution and stirred for 15 mins. The reaction was dissolved in ether (50 mL) and washed with water

(2X50 mL) then with brine (50 mL). The organic layer was extracted. The separated ether phase was washed with brine and purified by flash chromatography (Hexane/ethyl acetate (EtOAc) 10/1) to give a colorless oil.

#### **5-(4-butoxybenzylidene)-2,2-dimethyl-1,3-dioxane-4,6-dione (22)**

<sup>1</sup>H NMR (300 MHz, CDCl<sub>3</sub>): 8.37 (s, 1H), 8.23-8.21 (d, J=8.96, 2H), 6.97-6.95 (d, J=9.0 Hz, 2H), 4.09-4.06 (t, J=6.48 Hz, 2 H), 1.78 (s, 6H), 1.55-1.49 (q, J=7.2 Hz, 2 H), 1.01-0.97 (t, J=7.4, 3 H), 1.76-1.74 (d, J=7.0 Hz, 2 H), 1.72 (s, 3H), 1.50-1.44 (m, 5H)

#### **5-(4-butoxybenzyl)-2,2-dimethyl-1,3-dioxane-4,6-dione (23)**

<sup>1</sup>H NMR (300 MHz, CDCl<sub>3</sub>): 7.23-7.21 (d, J=8.64 Hz, 2H), 6.81-6.79 (d, J=8.64), 3.93-3.90 (t, J=6.52 Hz, 2H), 3.73-3.70 (t, J=4.84 Hz, 1H), 3.44-3.42 (d, J=4.84 Hz, 2H)

#### **3-butoxy-propionaldehyde (24)**

<sup>1</sup>H NMR (400 MHz, CDCl<sub>3</sub>): 9.81 (s, 1 H), 7.10-7.08 (d, J=8.6 Hz), 6.83-6.81 (d, J=8.6 Hz, 2H), 3.95-3.92 (t, J=6.52, 2H), 2.92-2.88 (t, J=7.48, 2H), 2.76-2.72 (t, J=8.44, 2H), 1.77-1.71 (q, J=7.12 Hz, 2H), 1.55-1.43 (m, 3H), 0.99-0.95 (t, J=7.4 Hz, 3H)

DMSO (14.0 mmol) was added dropwise to a stirred solution of oxalyl chloride (5.0 mmol) in DCM (20.0 mL) at 78 C and the resulting reaction mixture was stirred for 20 min at this temperature. Then cyclopropyl-propanol or cyclopropyl-propanol (4.0 mmol) was added dropwise and stirred for 1 h followed by the addition of Et<sub>3</sub>N (1.0 mL). The reaction was gradually brought to room temperature and H<sub>2</sub>O was added. The separated DCM phase was washed with brine and purified by flash chromatography (Hexane/ 1007 ethyl acetate (EtOAc): 10/1) to give a colorless oil.

#### **3-Cyclopropyl-propionaldehyde (31 a)**

<sup>1</sup>H NMR (400 MHz, CDCl<sub>3</sub>): d 9.80 (t, J = 1.8 Hz, 1H), 2.55-2.51 (m, 2H), 1.57-1.51 (m, 2H), 0.71-0.67 (m, 1H), 0.48e0.43 (m, 2H), 0.07-0.04 (m, 2H).

#### **3-Cyclohexyl-propionaldehyde (31 b)**

<sup>1</sup>H NMR (400 MHz, CDCl<sub>3</sub>): d 9.77-9.76 (t, J = 1.9 Hz, 1H), 1011 2.45-2.41 (t, J = 7.5, 1.9 Hz, 2H), 1.71-1.55 (m, 5H), 1.51-1.49 (m, 2H), 1.26-1.11 (m, 4H), 0.93-0.86 (m, 2H).

Maleimide (1 mmol) and triphenylphosphine (1 mmol) in acetone (10 mL) was refluxed for 1 hour. The formed precipitates were collected by sucking filtration and washed with acetone. Yield, 65%.

### **3-(3-phenylpropylidene)pyrrolidine-2,5-dione (40)**

<sup>1</sup>H-NMR(400 MHz, CDCl<sub>3</sub>): δ 7.63- 7.52 (m, 15 H), 3.03 (s, 2 H), 1.6536 (s, 2 H)

Aromatic aldehyde (1 mmol), triphenylphosphoranylidene succinimide (1 mmol) and methanol were added a flask. The reaction mixture was stirred at reflux temperature for 1.5 hours. Yield, 45%.

**3-(3-phenylpropylidene)pyrrolidine-2,5-dione (41):** <sup>1</sup>H-NMR(400 MHz, CDCl<sub>3</sub>)δ 7.31-7.15 (m, 5H), 6.86-6.81 (m, 1H), 3.01 (s, 2H), 2.83-2.80 (t, J=7.36, 2H), 2.52-2.47 (q, J=7.44, 2H)

A toluene solution of the Mitsunobu reagent, DIAD (1.5 mmol), was added dropwise to a THF solution of triphenylphosphine (1.5 mmol), maleimide derivative (1 mmol) and 2-tert-butoxycarbonylaminoethanol at room temperature. The reaction was stirred overnight. Solvent was removed under pressure and pure product was obtained by column chromatography. The Boc-protected compound (1 mmol) was dissolved in ethylacetate (3 mL). Dioxane-HCl (1 mmol) was added to the flask and the reaction was stirred for 2 hrs. Solid suspension was observed, the mixture was filtered and the collected solid washed with ethyl acetate and ether. Yield, 72%.

### **(2-(2,5-dioxo-3-(3-phenylpropylidene)pyrrolidin-1-yl)ethanaminium chloride (43)**

<sup>1</sup>H-NMR(400 MHz, MeOD): δ 7.30-7.17 (m, 5H), 6.83-6.78 (t, J=6.6 Hz, 1H), 3.85-3.81 (t, J=7.6 Hz, 2H), 3.183-3.130 (m, 4H), 2.86- 2.81 (t, J=7.5, 2H), 2.60-2.53 (q, J=7.8 Hz, 2H).

Preparation of N-alkylated oxindole: A mixture of 2-bromoethylamine hydrobromide (0.1 mmol) and analine (0.2 mmol) in 40 mL of toluene was heated at reflux for 16 hrs and then cooled. A solution of 60 mL of water and 20 mL of 50% aqueous KOH was added, and the layers were separated. The aqueous solution was saturated with NaCl and extracted thrice with dichloromethane. The combined organic layers were washed with saturated NaCl solution, dried over anhydrous Na<sub>2</sub>SO<sub>4</sub>, filtered and evaporated to dryness. Column chromatography gave the pure product. Yield, 60%.

### **N<sup>1</sup>-phenylethane-1,2-diamine (33):**

<sup>1</sup>H (400 MHz, MeOH): δ 7.10-7.08 (t, J=3.4 Hz, 2H), 6.67-6.60 (m, 3H), 3.23-3.20 (t, J= 6.08 Hz, 2H), 2.90-2.87 (t, J=6.24 Hz, 2H).

A solution of N-phenylethylenediamine and of di-t-butylcarbonate in methanol was stirred for 4 hrs and then concentrated by rotary evaporation to afford brown oil. Pure white solid was obtained from column chromatography.

**tert-butyl (2-(phenylamino)ethyl)carbamate (34)**

<sup>1</sup>H NMR (400 MHz, CDCl<sub>3</sub>): δ 7.25-7.18 (m, 2H), 6.81-6.6 (m, 2H), 3.38-3.36 (d, J=7.6 Hz, 2H), 3.27-3.23 (t, J=8.0 Hz, 2H), 1.48 (s, 9H)

A solution of SM, and triethylamine in dichloromethane was cooled to 0°C. Chloroacetyl chloride was added dropwise and the reaction was maintained at 0°C with stirring. After 3 hrs, another portion of chloroacetyl chloride was added dropwise. After 30 min, the reaction was poured into ethyl acetate and washed with water, saturated aqueous ammonium chloride, saturated aqueous sodium bicarbonate solution and brine. The solution was dried over sodium sulfate, filtered and concentrated in vacuum giving brown oil, chloroacetamide. Yield, 48%.

**tert-butyl (2-((chlorocarbonyl)(phenyl)amino)ethyl)carbamate (35)**

<sup>1</sup>H NMR (400 MHz, CDCl<sub>3</sub>): δ 7.48-7.41 (m, 3H), 7.28-7.27 (d, J=6.6 Hz, 2H), 3.87-3.83 (m, 4H), 3.35-3.34 (d, J=5.44 Hz, 2H), 1.4165 (s, 9H)

An oven dried two-mouthed flask equipped with a magnetic stirrer was evacuated while hot and cooled under nitrogen. The tube was charged with palladium acetate (5%), 2-(di-*tert*-butylphosphino) biphenyl (Pd: ligand = 2:1), and chloroacetanilide (1 mmol). The tube was evacuated and backfilled with nitrogen. Anhydrous triethylamine (1.5 mmol) was added, followed by anhydrous anhydrous toluene (1.0 mL). The septum was replaced was replaced under a positive pressure of nitrogen, and the sealed tube was placed in an oil bath preheated to 80°C. After 16 hours, the reaction was allowed to cool to room temperature and was diluted with ethyl acetate (10 mL). The mixture was filtered through a plug of Celite and concentrated on a rotary evaporator. The crude material thus obtained was purified by silica gel chromatography to give product oxindole. Yield, 65%.

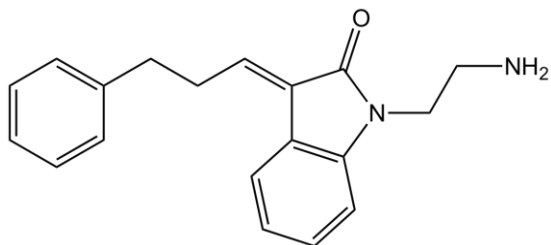
**tert-butyl (2-(2-oxoindolin-1-yl)ethyl)carbamate (36):**

<sup>1</sup>H NMR (400 MHz, CDCl<sub>3</sub>): δ 7.28-7.21 (m, 2H), 7.04-7.00 (t, J=7.5 Hz, 1H), 6.96-6.93 (d, 7.8 Hz, 1H), 4.14-4.07 (d, J= 7.2 Hz, 2H), 3.86-3.82 (t, J= 8.0Hz, 2H), 3.39-3.35 (q, J=5.7 Hz, 2H), 1.40 (s, 9H).

Various aldehydes (1.5 mmol) and piperidine (0.3 mmol) were added to a suspension of oxindole (1 mmol) in ethanol (15 mL). The solution was heated at 80°C for 1.5 hours. The reaction was allowed to cool to room temperature. The precipitate was filtered, was in ethanol. The Boc-protected compound (1 mmol) was dissolved in ethylacetate (3 mL). Dioxane-HCl (1 mmol) was added to the flask and the reaction was stirred for 2 hrs. Solid suspension was observed, the mixture was filtered and the collected solid washed with ethyl acetate and ether.

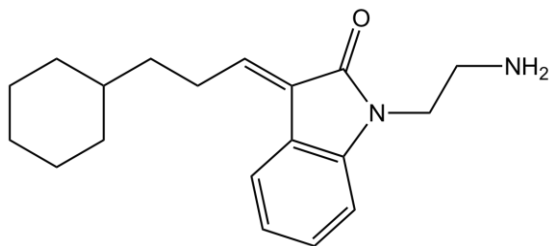
**1-(2-aminoethyl)-3-(3-phenylpropylidene)indolin-2-one (2):**  $^1\text{H}$  NMR (400 MHz, DMSO):  $\delta$  8.12 (s, 3H), 7.67-7.65 (d,  $J=7.52$  Hz, 1H), 7.35- 7.2890 (m, 5H), 7.23-7.20 (m, 2H), 7.10-7.06 (t,  $J=6.96$  Hz, 1H), 6.90-6.86 (t,  $J=7.24$  Hz, 1H), 4.00-3.96 (t,  $J=6.48$  Hz, 2H), 3.05- 2.99 (m, 4H), 2.95-2.91 (m, 2H).

$^{13}\text{C}$  NMR (100 MHz, DMSO): 167.0, 142.1, 140.7, 129.1, 128.4, 127.3, 126.1, 123.6, 122.2, 121.6, 108.7, 37.0, 36.6, 33.7, 30.1



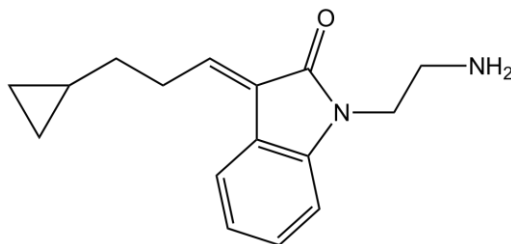
**1-(2-aminoethyl)-3-(3-cyclohexylpropylidene)indolin-2-one (3):**  $^1\text{H}$  NMR (400 MHz, DMSO):  $\delta$  8.1279 (s, 3H), 7.65-7.63 (d,  $J=7.48$ , 1H), 7.35-7.31 (t,  $J=7.2$  Hz, 1H), 7.22-7.20 (d,  $J=7.72$  Hz, 1H), 7.11-7.07 (t,  $J=8.16$  Hz, 1H), 6.90-6.86 (t,  $J=7.76$  Hz, 1H), 4.01-3.98 (t,  $J=6.48$ , 2H), 3.03-3.00 (m, 2H), 2.71-2.65 (q,  $J=7.64$  Hz, 2H), 1.74-1.51 (m, 5H), 1.49-1.39 (q,  $J=7.56$  Hz, 2H), 1.26-1.11 (m, 4H), 0.97-0.88 (m, 2H)

$^{13}\text{C}$  NMR (100 MHz, DMSO): 167.1, 142.2, 142.2, 128.9, 128.4, 126.8, 123.4, 122.2, 121.8, 108.7, 36.8, 36.7, 35.5, 32.6, 30.7, 26.1, 25.7



**1-(2-aminoethyl)-3-(3-cyclopropylpropylidene)indolin-2-one (4)**  $^1\text{H}$  NMR (400 MHz, MeOD):  $\delta$  7.35-7.33 (d,  $J$ = 6.88 Hz, 1H), 7.35-7.33 (t,  $J$ =6.84 Hz, 1H), 7.16-7.07 (m, 3H), 4.11-4.08 (t,  $J$ =6.00 Hz, 2H), 3.27-3.24 (t,  $J$ =5.72 Hz, 3H) 2.88-2.83 (q,  $J$ =7.44 Hz, 2H), 1.60-1.55 (q,  $J$ =7.16 Hz, 2H), 0.51-0.46 (m, 2H), 0.16-0.12 (m, 2H)

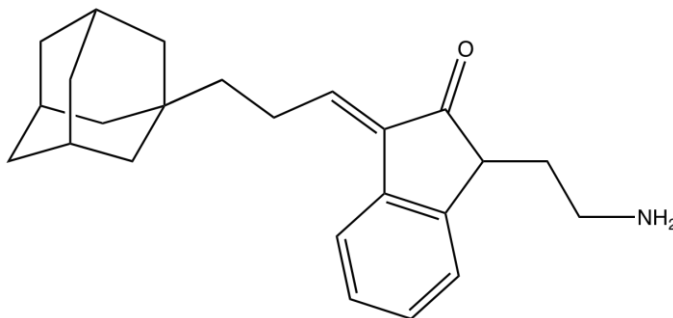
$^{13}\text{C}$  NMR (100 MHz, DMSO): 170.5, 144.4, 143.1, 130.2, 128.5, 125.1, 124.0, 123.7, 109.4, 39.3, 38.7, 34.8, 30.6, 11.7, 5.2.



**3-(3-((3*r*,5*r*,7*r*)-adamantan-1-yl)propylidene)-1-(2-aminoethyl)indolin-2-one (5)**

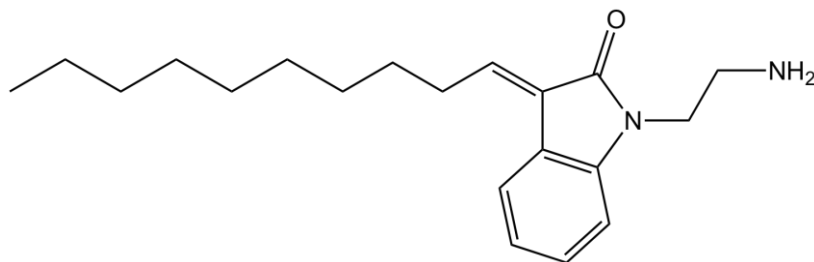
$^1\text{H}$  NMR (400 MHz, DMSO):  $\delta$  8.11 (s, 1H), 7.62-7.61 (d,  $J$ = 7.52 Hz, 1H), 7.35-7.31 (t,  $J$ =7.72 Hz, 1H), 7.22-7.20 (d,  $J$ =7.84 Hz, 1H), 7.12-7.09 (t,  $J$ =7.52 Hz, 1H), 6.91-6.87 (t,  $J$ =7.84 Hz, 1H), 4.00-3.97 (t,  $J$ =6.56, 2H), 3.04-3.00 (q,  $J$ =5.44, 2H), 2.65-2.59 (q,  $J$ =8.04 Hz, 2H), 1.99 (s, 3H), 1.71-1.60 (q,  $J$ =12.04 Hz, 6H), 1.54 (s, 6H), 1.36-1.32 (m, 2H).

$^{13}\text{C}$  NMR (100 MHz, DMSO): 167.0, 157.1, 142.1, 140.9, 132.4, 129.3, 129.0, 127.2, 123.5, 122.2, 121.6, 114.4, 114.3, 108.7, 67.0, 66.3, 37.0, 36.6, 32.8, 30.8, 30.4, 18.7, 13.7.



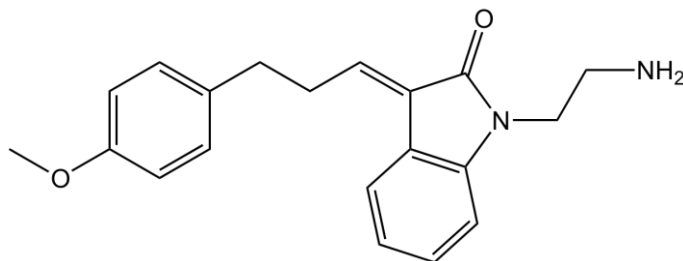
**1-(2-aminoethyl)-3-nonylideneindolin-2-one (6):**  $^1\text{H}$  NMR (400 MHz, DMSO):  $\delta$  7.96 (s, 1H), 7.67-7.65 (d,  $J$  = 7.56, 1H), 7.34-7.17 (t,  $J$  = 7.68, 1H), 7.17-7.16 (d,  $J$  = 7.8, 3H), 7.11-7.07 (t,  $J$  = 7.56, 1H), 6.91-6.87 (t,  $J$  = 7.80, 1H), 3.99-3.96 (t,  $J$  = 6.32, 2H), 2.71-2.65 (q,  $J$  = 7.40, 2H), 1.61-1.57 (m, 2H), 1.39-1.26 (m, 11H), 0.87-0.83 (t,  $J$  = 6.60, 3H).

$^{13}\text{C}$  NMR (100 MHz, DMSO): 142.1, 129.0, 127.0, 123.5, 122.2, 121.7, 36.8, 31.2, 28.8, 28.6, 28.0, 22.0, 13.9.



**1-(2-aminoethyl)-3-(3-(4-methoxyphenyl)propylidene)indolin-2-one (7)**  $^1\text{H}$  NMR (400 MHz, DMSO):  $\delta$  8.14 (s, 1H), 7.65-7.64 (d,  $J$  = 7.48, 1H), 7.35-7.31 (t,  $J$  = 7.72, 1H), 7.24-7.20 (t,  $J$  = 8.48, 3H), 7.10-7.06 (t,  $J$  = 7.60, 1H), 6.89-6.85 (m, 3H), 4.00-3.96 (t,  $J$  = 6.52, 2H), 3.01-2.95 (m, 4H), 2.88-2.85 (t,  $J$  = 6.92, 2H), 2.51-2.49 (m, 3H)

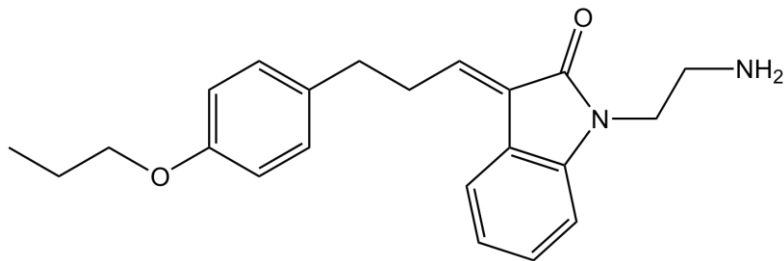
$^{13}\text{C}$  NMR (100 MHz, DMSO): 167.0, 157.7, 142.1, 141.9, 140.9, 140.6, 132.6, 129.3, 129.2, 129.1, 128.7, 127.2, 123.5, 122.2, 121.8, 121.6, 119.4, 113.8, 108.7, 108.4, 55.0, 37.0, 36.8, 36.8, 36.6, 33.4, 32.8, 30.4, 30.4, 29.3





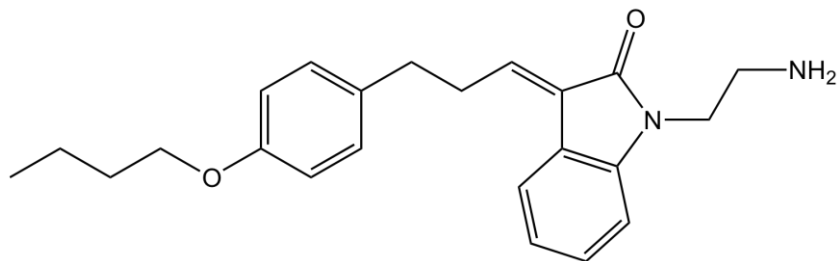
**1-(2-aminoethyl)-3-(3-(4-ethoxyphenyl)propylidene)indolin-2-one (8)**  $^1\text{H}$  NMR (400 MHz, DMSO):  $\delta$  8.14 (s, 1H), 7.65-7.64 (d,  $J$  = 7.48, 1H), 7.33-7.31 (t,  $J$  = 7.72 Hz, 1H), 7.24-7.20 (m, 3H), 7.10-7.06 (t,  $J$  = 7.60 Hz, 1H), 6.89-6.85 (m, 3H), 4.00-3.96 (t,  $J$  = 6.52, 2H), 4.00-3.96 (t,  $J$  = 6.52 Hz, 3H), 3.01-2.95 (m, 4H), 2.88-2.85 (t,  $J$  = 6.92 Hz, 2H), 2.51-2.49 (m, 3H)

$^{13}\text{C}$  NMR (100 MHz, DMSO): 167.1, 142.1, 132.4, 129.3, 129.0, 127.2, 123.6, 121.7, 114.2, 108.6, 62.9, 37.1, 36.8, 32.8, 30.4, 14.7



**1-(2-aminoethyl)-3-(3-(4-butoxyphenyl)propylidene)indolin-2-one (9)**  $^1\text{H}$  NMR (400 MHz, DMSO):  $\delta$  8.16 (s, 1H), 7.66-7.64 (d,  $J$  = 7.48 Hz, 1H), 7.35-7.31 (t,  $J$  = 7.72 Hz, 1H), 7.22-7.16 (m, 3H), 7.08-7.07 (t,  $J$  = 6.92 Hz, 1H), 6.89-6.84 (m, 3H), 4.00-3.97 (t,  $J$  = 6.56 Hz, 2H), 3.94-3.91 (t,  $J$  = 6.44 Hz, 3H), 3.03-2.95 (m, 4H), 2.87-2.84 (t,  $J$  = 6.96, 2H), 1.70-1.63 (m, 2H), 1.45-1.39 (m, 2H), 0.94-0.90 (t,  $J$  = 7.36 Hz, 3H)

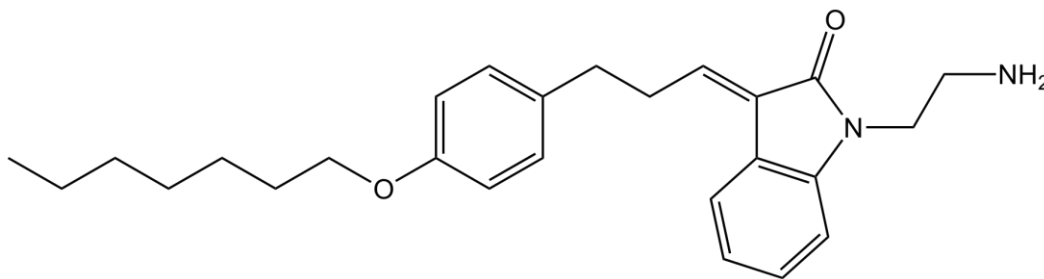
$^{13}\text{C}$  NMR (100 MHz, DMSO): 167.1, 142.9, 142.1, 128.9, 126.5, 123.3, 122.2, 121.7, 108.7, 66.3, 108.7, 37.0, 36.7, 36.6, 36.5, 32.0, 28.0, 22.4



**1-(2-aminoethyl)-3-(3-(4-(heptyloxy)phenyl)propylidene)indolin-2-one (10)**

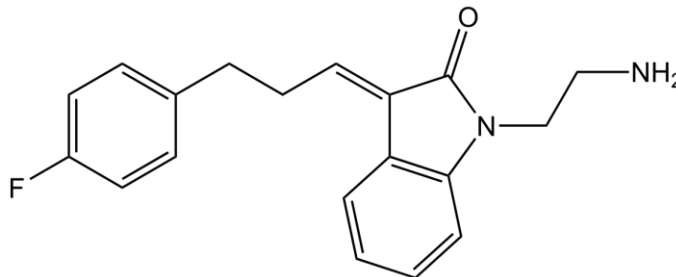
$^1\text{H}$  NMR (400 MHz, DMSO):  $\delta$  8.06 (s, 1H), 7.66-7.64 (d,  $J$ = 7.48 Hz, 1H), 7.35-7.31 (t,  $J$ =7.72 Hz, 1H), 7.22-7.18 (m, 3H), 7.10-7.06 (t,  $J$ =7.56 Hz, 1H), 6.89-6.84 (m, 3H), 3.99-3.95 (t,  $J$ =6.32, 2H), 3.93-3.90 (t,  $J$ =6.52 Hz, 3H), 3.02-2.95 (m, 4H), 2.87-2.84 (t,  $J$ =7.04 Hz, 2H), 1.72-1.65 (m, 2H), 1.43-1.17 (m, 8H), 0.88-0.85 (t,  $J$ =6.64 Hz, 3H)

$^{13}\text{C}$  NMR (100 MHz, DMSO): 167.0, 157.1, 142.1, 140.9, 132.4, 129.3, 129.0, 127.2, 123.6, 122.2, 121.7, 114.4, 108.6, 37.0, 36.7, 32.8, 31.2, 30.4, 28.7, 28.7, 28.4, 25.5, 22.0, 13.9.



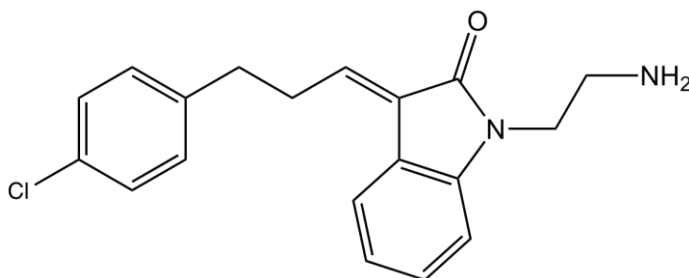
**1-(2-aminoethyl)-3-(3-(4-fluorophenyl)propylidene)indolin-2-one (11):**  $^1\text{H}$  NMR (400 MHz, MeOD):  $\delta$  7.66-7.64 (d,  $J$ =7.56, 1H), 7.35- 7.27 (m, 3H), 7.13-6.97 (m, 5H), 7.10-7.06 (t,  $J$ =6.96 Hz, 1H), 6.90-6.86 (t,  $J$ =7.24 Hz, 1H), 4.09-4.06 (t,  $J$ =5.88 Hz, 2H), 3.26- 3.23 (t,  $J$ =6.12 Hz, 2H), 3.08-3.03 (m, 2H), 2.99-2.95 (m, 2H).

$^{13}\text{C}$  NMR (100 MHz, DMSO): 170.0, 164.2, 161.8, 143.1, 138.0, 131.2, 130.4, 129.0, 125.0, 124.1, 123.5, 116.3, 116.1, 109.5, 39.3, 38.7, 34.6, 32.1



**1-(2-aminoethyl)-3-(3-(4-chlorophenyl)propylidene)indolin-2-one (12)**  $^1\text{H}$  NMR (400 MHz, DMSO):  $\delta$  7.97 (s, 3H), 7.67-7.65 (d,  $J=7.52$  Hz, 1H), 7.36- 7.32 (m, 5H), 7.17-7.15 (d,  $J=7.80$  Hz, 2H), 7.10-7.06 (t,  $J=6.96$  Hz, 1H), 6.87-6.84 (t,  $J=7.04$  Hz, 1H), 3.98-3.94 (t,  $J=6.28$  Hz, 2H), 3.04- 2.99 (m, 4H), 2.95-2.91 (m, 2H).

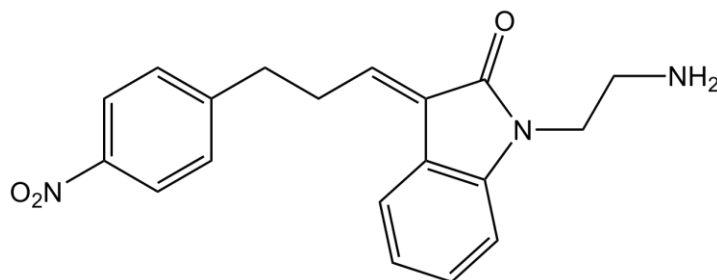
$^{13}\text{C}$  NMR (100 MHz, DMSO): 140.4, 139.8, 130.7, 129.1, 128.3, 127.4, 123.6, 122.2, 121.6, 108.7, 37.1, 36.7, 33.0, 29.9



**1-(2-aminoethyl)-3-(3-(4-nitrophenyl)propylidene)indolin-2-one (13)**

$^1\text{H}$  NMR (400 MHz, MeOD):  $\delta$  8.75-8.74 (d,  $J=7.48$  Hz, 3H), 7.67-7.65 (d,  $J=7.52$  Hz, 1H), 7.35- 7.2890 (m, 5H), 7.23-7.20 (m, 2H), 7.10-7.06 (t,  $J=6.96$  Hz, 1H), 6.90-6.86 (t,  $J=7.24$  Hz, 1H), 4.00-3.96 (t,  $J=6.48$  Hz, 2H), 3.05- 2.99 (m, 4H), 2.95-2.91 (m, 2H).

$^{13}\text{C}$  NMR (100 MHz, DMSO):  $\delta$  168.7, 147.4, 145.1, 135.1, 131.2, 129.9, 123.8, 124.2, 123.2, 115.6, 109.5, 37.9, 38.7, 26.6, 32.1



### **5.1 Cell Proliferative Assay**

The technique is based on the tetrazolium ring of 3-[4, 5-dimethylthiazol-2-yl]-2, 5-diphenyltetrazolium (MTT) that is cleaved by mitochondria reductase in living cells to produce a purple formazan. The purple formazan dissolved in DMSO is quantified at 540 nm. The assay reflects the number of viable cells, since reduction can only be stimulated by activated mitochondrial enzyme. The U937 cells were seeded at a density of  $2 \times 10^5$ , and 100  $\mu\text{L}$  of cells were added per well in a 96-well plate with a multi-channel pipette. The cells were treated with 100  $\mu\text{L}$  of active compounds at the concentration: 0, 1, 3, 10 and 30  $\mu\text{L}$ . 10  $\mu\text{L}$  of 5mg/ mL of (3-(4,5-Dimethylthiazol -2-yl)-2,5-diphenyltetrazolium bromide was added to each well and allowed to incubate at 37°C in a fully humidified atmosphere containing 5%  $\text{CO}_2$ . After which 170  $\mu\text{L}$  of medium was extracted from each well, and 100  $\mu\text{L}$  DMSO was added and mixed thoroughly to ensure homogeneity. The intracellular soluble formazan produced by the cellular reduction of the MTT was determined by recording the absorbance of each 96-well plate using the automatic microplate photometer (Flexstation3, Molecular Device, USA) at wavelength 570 nm. The values were expressed as percentage relative to those obtained in untreated controls. The  $\text{IC}_{50}$  was determined by constructing a dose-response curve.

## **5.2 Western Blot Assay**

Cells ( $5 \times 10^5$ /mL) were pretreated with compounds for 1 h, prior to being lysed by sonication in 1x sample buffer [62.5 mM Tris base (pH 6.8), 2% SDS, 50 mM DTT, 10% glycerol, 0.1% bromphenol blue, and 5 mg/mL each chymostatin, leupeptin, aprotinin, pepstatin, and soybean trypsin inhibitor] and boiled for 5 min. For analysis of phosphoproteins, 1 mM of sodium orthovanadate and sodium pyrophosphate was added to the sample buffer. Protein samples were collected from the supernatant after centrifugation of the samples at 12,800 g for 5 min, and protein was quantified using Coomassie Protein Assay Reagent.

Equal amounts of protein (30.0 mg) were separated by SDS-PAGE on 4-10% tris/glycine gel (Bio-Rad) and electrotransferred onto a PVDF membrane (Bio-Rad). For blotting phospho-proteins, no SDS was included in the transfer buffer. The blots were blocked with 5% milk in TBS-Tween 20 (0.1%) at 25°C for 1 h and probed with the appropriate dilution of primary antibody overnight at 4 °C. The blots were washed twice in TBS-Tween 20 for 15 min then incubated with a 1:2000 dilution of horseradish peroxidase conjugated secondary antibody in 5% milk/PBS-Tween 20 at 25°C for 1 h. After washing twice in TBS-Tween 20 for 15 min, the proteins were visualized by Western Blot Chemiluminescence Reagent. The primary antibodies used: Phospho-p44/42 MAPK (Thr202/Tyr204) antibody (1:1000, rabbit polyclonal), p44/42 MAPK antibody (1:1000, rabbit polyclonal), phospho-MEK1/2 (1:1000, rabbit polyclonal), MEK1/2 (1:1000, rabbit polyclonal), phospho-Akt(Ser473) (1:1000, rabbit polyclonal), (1:1000, rabbit

polyclonal), Akt1/2/3 (H-136) (1:1000, rabbit polyclonal).

### **5.3 Apoptosis assay**

After treatment with compounds at indicated concentrations for 24 hours, cells were washed twice with cold PBS and then suspended in 1x binding buffer (10 mM HEPES [N-2-hydroxyethylpiperazine-N-ethanesulfonic acid]/NaOH, pH 7.4, 140 mM NaOH, 2.5 mM CaCl<sub>2</sub>). The cells were incubated with annexin V fluorescein isothiocyanate (FITC) and 5mg/mL propidium iodide (PI), and incubated for 15 min at room temperature in the dark per the manufacturer's instructions. The samples were analyzed by flow cytometry using a Becton Dickinson FACScan within 1 h to determine the percentage of cells displaying annexin V staining (early apoptosis) or both annexin V and PI staining (late apoptosis).

## 6. Reference

1. Steelman, L. S.; Chappell, W.H. Roles of the Raf/MEK/ERK and PI3K/PTEN/Akt/mTOR pathways in controlling growth and sensitivity to therapy-implications for cancer and aging. *Aging*. **2011**, *3*, 192-222.
2. Evan, G. I.; Vousden, K. H. Proliferation, cell cycle and apoptosis in cancer. *Nature*. **2011**, *41*, 342-348.
3. Dhillon, A. S.; Hagan, S. R.; Rath, O.; Kolch, W. MAP kinase signaling pathway in cancer. *Oncogene*. **2007**, *6*, 3291-3310.
4. Schubbert, S.; Shannon, K.; Bollag, G. Hyperactive Ras in developmental disorders and cancer. *Nature Rev*. **2007**, *7*, 295-308.
5. Roberts, P. J.; Der, C. J. Targeting the Raf-MEK-ERK mitogen-activated protein kinase cascade for the treatment of cancer. *Oncogene* **2007**, *6*, 3291–3310.
6. Gustin, J. P.; Cosgrove, D. Park, B. The PIK3CA gene as a mutated target for cancer therapy. *Curr. Cancer Drug Targets*. **2008**, *8*, 733-740.
7. Hanahan, D.; Weinberg, R. A. The hallmarks of cancer. *Cell*. **2000**, *100*, 57-70.
8. Manson, M. M. Inhibition of survival signaling by dietary polyphenols and indole-3-carbinol. *Eur. J. of Cancer* **2005**, *41*, 1842-1853.
9. Cakir, M.; Grossmann, A. B. Targeting MAPK (Ras/ERK) and PI3K/Akt pathways in pituitary tumorigenesis. *Expert Opin. Ther. Targets* **2009**, *13*, 1121-1134
10. Cox, A. D.; Der, C. J. Ras history: The saga continues. *Small GTPases*. **2010**, *1*, 2-27.
11. Zwick, E.; Bange, J.; Ullrich, A. tyrosine kinase signalling as a target for cancer intervention strategies. *Endocr. Relat. Cancer* **2001**, *8*, 161–173.
12. Egan, S. E.; Giddings, B. W.; Brooks, M. W. Buday, L. Association of Sos Ras exchange protein with Grb2 is implicated in tyrosine kinase signal transduction and transformation. *Nature*. **1993**, *363*, 45 – 51.
13. Rude, B.; Voldborg, L.; Damstrup, M.; Skovgaard Poulsen, H. Epidermal growth factor receptor (EGFR) and EGFR mutations, function and possible role in clinical trials. *Anal. Oncol*. **1997**, *8*, 1197-1206.
14. Sirvent, A.; Benistant, C.; Roche, S. Cytoplasmic signalling by the c-Abl tyrosine kinase in normal and cancer cells. *Biol. Cell*. **2008**, *100*, 617–631.
15. Guo, J. Q.; Lian, J. Y.; Xian, Y. M. BCR protein expression in peripheral blood cell of chronic myelogenous leukemia patient undergoing therapy. *Blood*. **1994**, *2*, 3629-3637.
16. Blune-Jensen, P.; Hunter, T. Oncogenic kinase signaling. *Nature* **2001**, *411*, 355-365.
17. Milburn, M. V.; Tong, L. Biochemistry X-ray crystal structures of transforming p21 ras mutants suggest a transition-state stabilization mechanism for GTP hydrolysis. *Proc. Natl. Acad. Sci*. **1992**, *89*, 3649-3653.
18. Malumbres, M.; Barbacid, M. RAS oncogenes: the first 30 years. *Nature Rev. Cancer* **2003**, *3*, 459-465.

19. Steelman, L. S.; Ponher, S. C. Shelton, J. G. Franklin, R. A. JAK/STAT, Raf/MEK/ERK, PI3K/Akt and BCR-ABL in cell cycle progression and leukemogenesis. *Leukemia* **2004**, *18*, 189–218.
20. Chonga, H.; Vikisa, H. G. Guana, K-L. Mechanisms of regulating the Raf kinase family. *Cell. Signal.* **2003**, *15*, 463–469.
21. Alessi, D.; Salto, Y.; Campbell, D. G. Identification of the sites in MAP kinase kinase-1 phosphorylated by p74raf-1. *EMBO J.* **1994**, *13*, 1610-1619.
22. Ferrell, J.; Bhatt R. Mechanistic Studies of the dual phosphorylation of mitogen-activated protein kinase. *J. Biol. Chem.* **1997**, *272*, 19008-19016.
23. Steelman, L. S.; Franklin, R. A.; Abrams, S. L. Chappell, W. Kempf, C. R. Roles of the Ras/Raf/MEK/ERK pathway in leukemia therapy. *Leukemia*. **2011**, *25*, 1080–1094.
24. Yoon, S.; Seger, R. The extracellular signal-regulated kinase: multiple substrates regulate diverse cellular functions. **2006**, *24*, 21-44.
25. Roux, P. P.; Blenis, J. ERK and p38 MAPK-Activated Protein Kinases: a family of protein kinases with diverse biological functions. *Microbiol. Molec. Biol. Rev.* **2004**, *68*, 320-344.
26. Saini, K. S.; Piccart-Gebhart, M. J. Dual targeting of the PI3K and the MAPK pathways in Breast Cancer. *Asia Pac. J. Oncol. Hematol.* **2010**, *2*, 13-17.
27. Cantley, L. C. The phosphoinositide 3-kinase pathway. *Science* **2002**, *296*, 1655-1657.
28. Courtney, K.D. Corcoran, R. B.Engelman, J. A. The PI3K pathway as drug target in human cancer. *J. Clin. Oncol.* **2010**, *28*, 1075-1083
29. Karakas, B; Bachman, K. E.; Park, B. H. Mutation of the PIK3CA oncogene in human cancers. *B. J. Cancer.* **2006**, *94*, 455–459.
30. Carpenter, C.L.; Auger, K. R.; Chanudhuri, M. Phosphoinositide 3-kinase is activated by phosphopeptides that bind to the SH2 domains of the 85-kDa subunit. *J. Biol. Chem.* **1993**, *268*, 9478-9483.
31. Shaw R.J.; Cantley L.C. Ras, PI(3)K and mTOR signalling controls tumour cell growth. *Nature* **2006**, *441*, 424-430.
32. Hart, J. R.; Vogt, P. K. Phosphorylation of AKT: a Mutational Analysis. *Oncotarget* **2011**, *2*, 467-476.
33. Carpten, J. D.; Faber, A. L.; Horn, C. Donoho, G. P. A transforming mutation in the pleckstrin homology domain of AKT1 in cancer. *Nature* **2007**, *448*, 439-444.
34. Park, B. H.; Karakas, B.; Bachman, K. E. Mutation of the PIK3CA oncogene in human cancers. *Nat. Rev. Cancer* **2002**, *2*, 489-501.
35. Sengupta, S. Regulation of the mTOR complex 1 pathway by nutrients, growth factor and stress. *Mol. Cell.* **2010**, *40*, 310- 322.
36. Wu, P.; Hu, Y. Z. PI3K/AKT/mTOR pathway inhibitors in cancer: A perspective on clinical progress. *Curr. Med. Chem.* **2010**, *17*, 4326-434.
37. Zivny, J.; Klener, P. Pytilka, R.; Andera, L. Role of apoptosis in cancer development and dreatment: focusing on the development and treatment of hematologic malignancies. *Curr. Pharmaceut. Design* **2010**, *16*, 11-33.
38. Mendoza, E. Emrah, E.; Blenis, J. The Ras-ERK and PI3K-mTOR pathways: cross-talk and compensation. *Trends Biochem. Sci.* **2011**, *36*, 320-328



39. Harada, H.; Andersen, J. S.; Mann, M. p70S6 kinase signals cell survival as well as growth, inactivating the pro-apoptotic molecule BAD. *Proc. Natl. Acad.* **2001**, *98*, 9666-9670.
40. Kelly, P. N.; White, M. J. Goshnick, M. W. Individual and overlapping roles of BH3-only proteins Bim and Bad in apoptosis of lymphocytes and platelets and in suppression of thymic lymphoma development. *Cell Death Differ.* **2010**, *10*, 1655-1664.
41. Alan, L. A.; Morrice, N.; Brady, S. Inhibition of caspase 9 through phosphorylation at Thr125 by ERK MAPK. *Nat. Cell. Biol.* **2003**, *5*, 647-654.
42. Lee, T.; Guang, Y.; Nevins, J.; You, L. Sensing and integration of Erk and PI3K signals by myc. *PLoS. Comput Biol.* **2008**, *4*, (9 pages).
43. Shelton, J. G.; Steelman, L. S.; White, E. R.; McCubrey, J. A. Synergy between PI3K/Akt and Raf/MEK/ERK Pathways in IGF- 1R mediated cell cycle progression and prevention of apoptosis in hematopoietic cells. *Cell Cycle* **2004**, *3*, 372-379.
44. Zhong, Z.; Yeow, W-S.; Zou, C. Cyclin D1/cyclin dependent kinase 4 interacts with filamin A and affects the migration and invasion potential of breast cancer cells. *Cancer Res.* **2010**, *70*, 2105-2114.
45. Ramakrishnan, M.; Musa, M. L.; Li, J. Catalytic activation of extracellular signal-regulated kinase induces cyclin D1 expression in primary tracheal myocytes. *Am. J. Respir. Cell Mol. Biol.* **1998**, *18*, 736-740
46. Chang, F.; Lee, J. T.; Novalanic, P. M. Involvement of PI3K/Akt pathway in cell cycle progression, apoptosis, and neoplastic transformation: a target for cancer chemotherapy. *Leukemia.* **2003**, *17*, 590–603.
47. Roberts, E.C.; Shapiro, P.S. Distinct cell cycle timing requirements for extracellular signal-regulated kinase and phosphoinositide 3-Kinase signaling pathways in somatic cell mitosis. *Mol Cell Biol.* **2002**, *22*, 7226–7241.
48. Pray, L. A. Gleevec: The breakthrough in cancer treatment. *Nature Ed.* **2008**, *1*, 1.
49. Manley, P. W.; Cowan-Jacob, S. W. Advances in the structural biology, design and clinical development of Bcr-Abl kinase inhibitors for the treatment of chronic myeloid leukemia. *Biochimica Biophysica Acta.* **2005**, *1754*, 3 – 13.
50. Wilhelm, S.; Carter, C.; Lynch, M.; Smith, R. A.; Schwartz, B.; Simantov, R. Discovery and development of sorafenib: a multikinase inhibitor for treating cancer. *Nat. Rev. Drug. Discov.* **2006**, *14*, 835-844.
51. Wilhelm, S. M.; Carter, C. BAY 43-9006 Exhibit broad spectrum oral antitumor activity and targets the RAF/MEK/ERK pathway and receptor tyrosine kinases involved in tumor progression and angiogenesis. *Cancer Res.* **2004**, *64*, 7099-7109.
52. Friday, B. B.; Adjei, A. A. Advances in targeting the Ras/Raf/MEK/Erk Mitogen-Activated Protein Kinase Cascade with MEK inhibitors for cancer therapy. *Clin Cancer Res.* **2008**, *14*, 342-346.
53. Yua, R.; Kay, A.; Berg, W. J.; Lebwohl, D. Targeting tumorigenesis: development and use of mTOR inhibitors in cancer therapy. *J. Hematol. Oncol.* **2009**, *2*, 45-56.

54. Engelman, J. A. Targeting PI3K signalling in cancer: opportunities, challenges and limitation. *Nat Rev Cancer*. **2009**, *8*, 550-62.
55. Gills, J. J.; Dennis, P. A. Perifosine: Update on a novel Akt inhibitor. *Curr. Oncol. Rep.* **2009**, *11*, 102-110.
56. Kiyatkin, A.; Kholodenko, B. N.; Aksamitiene, E.; Kolch, W.; Hoek, J. B. PI3K/Akt-sensitive MEK-independent compensatory circuit of ERK activation in ER-positive PI3K-mutant T47D breast cancer cells. *Cell Signal.* **2010**, *22*, 1369-1378.
57. Wang, C; Cirit, M.; Haugh, J. M.; PI3K-dependent crosstalk interactions converge with Ras as quantifiable inputs integrated by Erk. *Mol. Syst. Biol.* **2009**, *5*, 246-257.
58. Sherr, C. J.; Weber, J. D. The ARF/p53 pathway. *Current Opinion in Genetics & Development.* **2000**, *10*, 94-99.
59. McCubrey, J. A.; Steelman, L. S.; Chappell, W. H. Abrams, S. L. Roles of the Raf/MEK/ERK pathway in cell growth, malignant transformation and drug resistance *Biochim. Biophys. Acta.* **2007**, *8*, 1263-1284.
60. Hancock, C. N.; Macias, A.; Lee, E. K.; Yu, S. Y.; Shapiro, P.S. Identification of novel extracellular signal-regulated kinase docking domain inhibitors. *J. Med. Chem.* **2005**, *48*, 4586-4595.
61. Li, Q.; Al-Ayoubi, A. Guo, T.; Zheng, H. Structure-activity relationship (SAR) studies of 3-(2-amino-ethyl)-5-(4-ethoxy-benzylidene)thiazolidine-2,4-dione: Development of potential substrate-specific ERK 1/2 inhibitors. *Bioorg. Med. Chem. Lett.* **2009**, *19*, 6042-6046.
62. Jones, G.; Willett, P.; Glen, R. C., Leach, A. R.; Taylor, R. Development and validation of a genetic algorithm for flexible docking. *J. Mol. Biol.* **1997**, *267*, 727-748.
63. Li, Q.; Wu, J.; Zheng, H.; Liu, K. Discovery of 3-(2-aminoethyl)-5-(3-phenyl-propylidene)-thiazolidine-2,4-dione as a dual inhibitor of the Raf/MEK/ERK and the PI3K/Akt signaling pathways. *Bioorg. Med. Chem. Lett.* **2010**, *20*, 4526-4530.

